Title

A variant erythroferrone disrupts iron homeostasis in SF3B1-mutated myelodysplastic syndrome.

Journal

Science Translational Medicine, 11(500)

Authors

Bondu, Sabrina
Alary, Anne-Sophie
Lefèvre, Carine
et al.

Publication Date

2019-07-10

DOI

10.1126/scitranslmed.aav5467

Peer reviewed

HHS Public Access

Author manuscript

Sci Transl Med. Author manuscript; available in PMC 2021 March 28.

Published in final edited form as:

Sci Transl Med. 2019 July 10; 11(500): . doi:10.1126/scitranslmed.aav5467.

A variant erythroferrone disrupts iron homeostasis in *SF3B1*-mutated myelodysplastic syndrome

Sabrina Bondu[1,2,3,4,†], **Anne-Sophie Alary**[1,2,3,4,5,†], **Carine Lefèvre**[1,2,3,4,6], **Alexandre Houy**[7], **Grace Jung**[8], **Thibaud Lefebvre**[6,9], **David Rombaut**[1,2,3,4], **Ismael Boussaid**[1,2,3,4], **Abderrahmane Bousta**[1,2,3,4], **François Guillonneau**[1,2,3,4,10], **Prunelle Perrier**[11], **Samar Alsafadi**[12], **Michel Wassef**[13], **Raphaël Margueron**[13], **Alice Rousseau**[1,2,3,4], **Nathalie Droin**[14], **Nicolas Cagnard**[15], **Sophie Kaltenbach**[16], **Susann Winter**[17], **Anne-Sophie Kubasch**[18], **Didier Bouscary**[19], **Valeria Santini**[20], **Andrea Toma**[21], **Mathilde Hunault**[22], **Aspasia Stamatoullas**[23], **Emmanuel Gyan**[24], **Thomas Cluzeau**[25], **Uwe Platzbecker**[18], **Lionel Adès**[26], **Hervé Puy**[6,9], **Marc-Henri Stern**[27], **Zoubida Karim**[6,9], **Patrick Mayeux**[1,2,3,4,6,10], **Elizabeta Nemeth**[8], **Sophie Park**[28], **Tomas Ganz**[8], **Léon Kautz**[11], **Olivier Kosmider**[1,2,3,4,5,6,*], **Michaëla Fontenay**[1,2,3,4,5,6,*]

[1]Institut Cochin, Department Development, Reproduction and Cancer, Paris 75014, France

[2]Institut National de la Santé et de la Recherche médicale (INSERM) U1016, Paris 75014, France

[3]Centre National de la Recherche Scientifique (CNRS) Unité Mixte de recherche (UMR) 8104, Paris 75014, France

[4]Université Paris Descartes, Sorbonne-Paris Cité, Paris 75006, France

[5]Assistance Publique-Hôpitaux de Paris, Hôpitaux Universitaires Paris Centre – Cochin, Service d'hématologie biologique, Paris 75014, France

[6]Laboratoire d'excellence du Globule Rouge GR-Ex, Université Paris Descartes, Paris 75015, France

[7]Department of Human Genetics and Oncogenesis, Institut Curie, Paris 75005, France

[8]Department of Medicine, David Geffen School of Medicine, University of California, Los Angeles, CA 90095, USA

[*]To whom correspondence should be addressed: olivier.kosmider@aphp.fr; michaela.fontenay@inserm.fr.

Author contributions: S.B., A-S.A., C.L., G.J., F.G., T.L., P.P., M.W., A.R. and L.K. performed the experiments and analyzed the data; AR, SW, A-SK, recorded patient clinical data; A.H., D.R., A.B., N.C. and I.B. performed bioinformatics analyses; A.T., S.P., D.B., H.P., L.A., U.P., T.C., M.H., A.S., and E.G. provided samples; S.P. performed statistical analyses and reviewed the manuscript; F.G., N.D., S.A., Z.K., H.P., M.W., R.M., M-H.S., P.M., E.N., T.G., L.K. analyzed the data and reviewed the manuscript; M.F. and O.K. designed the study, analyzed the data, supervised the work; M.F. wrote the manuscript.

[†]These authors equally contributed to the work.

Competing interests: T.G., L.K., and E.N. are inventors on a patent application on ERFE. T.G. and E.N. are scientific founders of Intrinsic LifeSciences and Silarus Pharma, companies that have interests related to ERFE. M.F., O.K., L.K., F.G., M-H.S., S.A., A.H. are inventors on a patent application on variant ERFE. The other authors have no competing interests to disclose.

Data and materials availability: RNA-seq data are available in the Gene Expression *Omnibus* (*GEO*) repository (accession number GSE113433). Material transfer agreement with H3 Biomedicine Inc. (Dr S Buonamici) is required to obtain synthetic full length *SF3B1*^{WT} or mutant *SF3B1*^{K700E} cDNAs. All other data associated with this study are present in the paper or the Supplementary Materials.

[9]INSERM, UMR 1149/ERL CNRS 8252, Centre de Recherches sur l'inflammation, Université Paris Diderot, Paris 75018, France

[10]Proteomic platform 3P5, Université Paris Descartes, Paris 75014, France

[11]Institut de Recherche en Santé Digestive (IRSD), Université de Toulouse, INSERM U1220, Institut National de la Recherche Agronomique U1416, Ecole Nationale Vétérinaire de Toulouse, Université Paul Sabatier, Toulouse 31024, France

[12]Institut Curie, PSL Research University, Department of Translational Research, Paris 75005, France

[13]Institut Curie, PSL Research University, INSERM 934/UMR 3215, Genetics and biology of Development, Paris 75005 France

[14]Institut Gustave Roussy, Genomic platform, Villejuif 94805, France

[15]Platform Bioinformatics, Paris Descartes University, Paris 75015, France

[16]Assistance Publique-Hôpitaux de Paris, Laboratoire de Génétique, Hôpital Necker, Paris 75015, France

[17]Medical Clinic und Policlinic 1, Technische Universität Dresden, Dresden 01307, Germany

[18]Medical Clinic und Policlinic 1, Hematology and Cellular Therapy, University Hospital, Leipzig 04103, Germany

[19]Assistance Publique-Hôpitaux de Paris, Hematology Department, Hôpital Cochin, and Paris Descartes University, Paris 75014, France

[20]MDS unit, Hematology, AOU Careggi, University of Florence, Florence 50134, Italy

[21]Assistance Publique-Hôpitaux de Paris, Hematology Department, Hôpital Henri-Mondor, and Paris 12 University, Créteil 94000, France

[22]Service des Maladies du Sang, Centre hospitalo-universitaires, Angers 49100, France

[23]Département d'hématologie, Centre Henri-Becquerel, Rouen 76038, France

[24]Service d'hématologie et thérapie cellulaire, Centre hospitalo-universitaire, CNRS ERL 7001 LNOx, Université de Tours, Tours 37044, France

[25]Côte d'Azur University, CHU of Nice, Hematology department and INSERM U1065, Mediterranean Center of Molecular Medecine, Nice 06204, France

[26]Assistance Publique-Hôpitaux de Paris, Service d'Hématologie Senior, Hôpital Saint-Louis, Paris 75010, France

[27]Institut Curie, Université de recherche PSL, Inserm U830, DNA repair and uveal melanoma (D.R.U.M.) and Département de génétique, Équipe labellisée par la Ligue nationale contre le cancer, Paris 75005, France.

[28]Department of Hematology, Centre Hospitalier Universitaire, Université de Grenoble Alpes, La Tronche 38700, France

Abstract

Myelodysplastic syndromes (MDS) with ring sideroblasts are hematopoietic stem cell disorders with erythroid dysplasia and mutations in the *SF3B1* splicing factor gene. MDS patients with *SF3B1* mutations often accumulate excessive tissue iron, even in the absence of transfusions, but the mechanisms that are responsible for their parenchymal iron overload are unknown. Body iron content, tissue distribution, and the supply of iron for erythropoiesis are controlled by the hormone hepcidin, which is regulated by erythroblasts through secretion of the erythroid hormone erythroferrone (ERFE). Here, we identified an alternative *ERFE* transcript in MDS patients with the *SF3B1* mutation. Induction of this *ERFE* transcript in primary *SF3B1*-mutated bone marrow erythroblasts generated a variant protein that maintained the capacity to suppress hepcidin transcription. Plasma concentrations of ERFE were higher in MDS patients with a *SF3B1* gene mutation than in patients with *SF3B1* wild-type MDS. Thus, hepcidin suppression by a variant erythroferrone is likely responsible for the increased iron loading in patients with *SF3B1*-mutated MDS, suggesting that ERFE could be targeted to prevent iron-mediated toxicity. The expression of the variant *ERFE* transcript that was restricted to *SF3B1*-mutated erythroblasts decreased in lenalidomide-responsive anemic patients, identifying variant ERFE as a specific biomarker of clonal erythropoiesis.

One Sentence Summary:

A variant erythroferrone contributes to hepcidin modulation and systemic iron accumulation in patients with *SF3B1*-mutated myelodysplastic syndrome.

Introduction

Myelodysplastic syndromes with ring sideroblasts (MDS-RS) are clonal hematopoietic stem cell (HSC) disorders with a prominent erythroid dysplasia of the bone marrow (BM) responsible for a macrocytic anemia. Mitochondrial iron accumulation and apoptosis of mature erythroblasts cause ineffective erythropoiesis (1, 2). In contrast to other MDS subtypes, patients with MDS-RS exhibit signs of systemic iron accumulation that is reflected by increased ferritin and non-transferrin bound iron concentrations even before they become transfusion-dependent and subsequently develop parenchymal iron overload (3, 4).

Splicing factor gene *SF3B1* is mutated in ~90% of MDS-RS, and the diagnosis is considered whenever the gene is mutated, even if the percentage of RS is relatively low, between 5 and 15% (5–7). These mutations arise in the HSCs (8–10). Aberrant splicing events are reported in MDS and other *SF3B1*-driven cancers, including uveal melanoma and chronic lymphocytic leukemia (CLL) (11–14). The selection of an alternative branch site resulting in the use of a cryptic 3’ splice site (ss) is the most frequently detected abnormality. Computational analysis revealed that the majority of cryptic 3’ss are located upstream of canonical 3’ss at nucleotide distances that are not multiples of 3, suggesting that the aberrant transcripts would likely contain a premature termination codon (PTC) and be degraded by non-sense mediated decay (NMD). It has been predicted that half of the aberrantly spliced transcripts in *SF3B1*-mutated cells are NMD-sensitive and that the canonical isoforms are down-regulated (11). For instance, *ABCB7* transcript encoding a mitochondrial transporter involved in the export of Fe-S clusters is aberrantly spliced and undergoes NMD. It is also possible that NMD-insensitive aberrant transcripts are translated into proteins with altered

function (11). Globally, mis-splicing may contribute to defective mRNA production and deregulation of cellular pathways (17–18). How these aberrant splicing events contribute to the disease phenotype and in particular to systemic iron overload is unclear.

In contrast with other MDS subtypes, MDS-RS are associated with lower expression of the iron homeostasis regulator, hepcidin, and as a consequence, the absorption of iron by duodenal enterocytes and its release from erythrophagocytic macrophages may be increased (19–24). Inappropriately low hepcidin concentrations in MDS-RS could depend on the degree of ineffective erythropoiesis linked to impaired iron incorporation into heme because of mitochondrial iron trapping and/or to increased expression of hepcidin repressors (25). Growth differentiation factor 15 (GDF-15) and twisted gastrulation (TWSG1), two members of the transforming growth factor-β superfamily, have been proposed as pathological suppressors of hepcidin in ineffective erythropoiesis (26, 27). More recently, erythroferrone (ERFE), a C1q–tumor necrosis factor–related family of proteins (CTRP) member, has been described as a major erythroid regulator of hepcidin, involved in the pathological suppression of hepcidin in patients with β-thalassemia (28, 29).

In the present study, we identify a variant transcript of *ERFE* specific to *SF3B1*-mutated MDS. The expression of the variant *ERFE* is restricted to the erythroid lineage, and the variant contributes to increased concentration of ERFE protein, resulting in hepcidin suppression and systemic iron accumulation in patients. This variant appears to be a pertinent biomarker of clonal erythropoiesis with potential use for monitoring treatment response of anemic patients with *SF3B1*-mutated MDS.

Results

Upregulation of ERFE using an alternative 3’ splice site in SF3B1-mutated MDS

To investigate the mechanism of systemic iron overload, we established a cohort of 156 patients with lower risk MDS, including 60 MDS-RS with single lineage dysplasia (SLD), 17 MDS-RS with multilineage dysplasia (MLD), 2 5q-syndrome, 17 MDS-SLD, 42 MDS-MLD, and 18 MDS with type 1 excess of blasts (EB1) (table S1). The Revised-International Prognosis Scoring System score was very low in 15, low in 95, intermediate in 36, and high in 4 patients. Twenty-six genes commonly mutated in MDS were sequenced in the BM mononuclear cell (MNC) fraction. *SF3B1* gene was mutated in 94 patients with MDS, including 63 (67%) affected by a *SF3B1*^{K700E} mutation. Among the 62 patients with no *SF3B1* mutation, other splicing genes, *SRSF2*, *U2AF1*, or *ZRSR2* were mutated in 27 cases, and no splicing gene mutation was observed in 35 cases. Some patients presented with two splicing mutations (fig. S1). We evaluated the consequences of *SF3B1* gene mutations on gene expression and splicing by sequencing the transcriptome of the BM MNCs isolated from 27 patients in this cohort, including 21 with *SF3B1*^{MUT} MDS, 6 with *SF3B1*^{WT} MDS, and 5 healthy controls. Differential analyses of gene expression and splice junctions were conducted using DESeq2 (30). We detected 6,343 genes as differentially expressed between *SF3B1*^{MUT} MDS and *SF3B1*^{WT} MDS with a *P*-value<0.05 (data file S1). Principal component analysis (PCA) of gene expression profiles separated *SF3B1*^{MUT} and *SF3B1*^{WT} MDS (Fig. 1A). The differentially expressed genes were enriched in 73 specific GO terms with an absolute $\log_2$ fold-change (FC)>1 and a Benjamini-Hochberg (BH)-adjusted *P*-

value<0.05 (Fig. 1B). Genes with a $\log_2$(FC)< −1 were involved in serine/threonine kinase signaling, apoptosis, myeloid differentiation, inflammation, and cell-cell adhesion, whereas those with a $\log_2$(FC)>1 were involved in heme metabolism, erythrocyte differentiation, and iron homeostasis (Fig. 1C). We plotted the $\log_2$(FC) of 16 differentially expressed genes belonging to the IRON_ION_HOMEOSTASIS gene set (GO:0055072; http://amigo.geneontology.org) and showed that the *FAM132B/ERFE* transcript encoding erythroferrone was increased (Fig. 1D). The *FAM132B/ERFE* transcript was similarly expressed in samples with an epigenetic $TET2^{MUT}/DNMT3A^{WT}/SF3B1^{WT}$ genotype compared to healthy controls or with a $DNMT3A^{MUT}/TET2^{WT}/SF3B1^{MUT}$ compared to $DNMT3A^{WT}/TET2^{WT}/SF3B1^{MUT}$ genotype, suggesting that the deregulation of *ERFE* transcript expression was linked to *SF3B1* mutation (table S2).

We then identified 1,528 differentially expressed 5’ and 3’ junctions, including annotated 5’ donor and 3’ acceptor ss, ambiguous junctions, and canonical junctions with BH-adjusted *P*-values $\leq 10^{-5}$ and absolute $\log_2$(FC) ≥1 (data file S2). These junctions allowed the hierarchical clustering of the 21 $SF3B1^{MUT}$ and 6 $SF3B1^{WT}$ MDS samples (Fig. 2A). After excluding differentially expressed canonical junctions, we then considered the 1,147 alternative junctions, among which we identified 786 3’ acceptor junctions (68.5%), 176 5’ donor junctions (15.3%), and 185 ambiguous junctions (16.1%) attributed to either the alternative 5’ or 3’ss or both alternative 5’ and 3’ss (Fig. 2B). The analysis of distances between the alternative and canonical 3’ss showed that the majority of alternative 3’ss (AG’) was located between −24 and −9 nucleotides preceding the canonical 3’ss (AG) (Fig. 2C). The proportion of alternative AG’ junctions in these novel splice variants was generally increased in *SF3B1* mutants and less frequently in $SF3B1^{WT}$ samples (Fig. 2D). To detect alternative transcripts that were likely to generate substantial amounts of variant proteins with a modified length, we applied a filter selecting transcripts with an additional stretch of nucleotides numbering in multiples of 3, a ratio of alternative junction coverage (AG’) to alternative and canonical junctions coverage (AG’+AG) over 0.1, and an expression ratio of the alternative junction in $SF3B1^{MUT}$ versus $SF3B1^{WT}$ samples over 10 (fig. S2A). We obtained 66 alternative junctions in 63 genes (data file S3 & fig. S2B). These genes were involved in the epigenetic regulation and transcription, mRNA processing and translation, intracellular transport, cell cycle and migration, signaling and apoptosis, mitochondrial metabolism, and iron homeostasis (Fig. 2E). Among the 66 alternative junctions, 29 were related to an in-frame insertion of 9 to 27 nucleotides, and 26 of them were differentially expressed between $SF3B1^{MUT}$ and $SF3B1^{WT}$ MDS with an absolute $\log_2$(FC) >0.3 (Fig. 2F). *FAM132B/ERFE* gene was identified among the upregulated genes with an alternative junction due to the use of a cryptic 3’ss located between exons 2 and 3 (chr2: 239,070,357 – 239,071,364) and no PTC. The aberrant transcript contained 12 additional nucleotides in the open reading frame and from here on is referred to as $ERFE^{+12}$ (Fig. 2G). It was systematically detected in all $SF3B1^{MUT}$ MDS samples and represented a mean percentage of 24.8% of *FAM132B/ERFE* transcripts in $SF3B1^{MUT}$ MDS versus 0.2% in $SF3B1^{WT}$ MDS. The mutation pattern of samples expressing $ERFE^{+12}$ is shown in fig. S2C. This indicates that the expression of $ERFE^{+12}$ was strongly linked to the presence of a mutation in *SF3B1* gene.

SF3B1^{MUT}-restricted expression of alternative ERFE^{+12} transcript

To ascertain that expression of the *ERFE*$^{+12}$ transcript is dependent on the presence of a *SF3B1* mutation, we transfected the erythro-megakaryocytic cell line UT7/EPO with a pLVX plasmid encoding a synthetic full-length *SF3B1*^{WT} or mutant *SF3B1*^{K700E} cDNA. We then designed a sensitive fluorescent PCR allowing the detection of *ERFE*$^{+12}$ and *ERFE*^{WT} transcripts as 162 nucleotides (nt) and 150 nt fragments by capillary electrophoresis (table S3). Twenty-four hours after transfection, *ERFE*$^{+12}$ transcript was detected in *SF3B1*^{K700E} transfected cells, but not in *SF3B1*^{WT} cells (Fig. 3A). To validate the splice pattern induced in the context of *SF3B1* mutation in *ERFE* pre-mRNA, we performed a minigene splicing assay. An *ERFE* sequence of about 200 nucleotides located on both sides of the cryptic 3'ss (AG') was cloned in an ExonTrap vector. The alternative junction in *ENOSF1* gene (chr18: 683,395–685,920) cloned in the same vector was used as a control (13). These minigenes were transfected into the murine G1E-ER4 cell line in which the *SF3B1*^{K700E} mutation was edited by CRISPR-Cas9 technology. As expected due to the lack of intron homology between species, sequencing the transcriptome of G1E-ER4 *SF3B1*^{K700E} cell line or isogenic *SF3B1*^{WT} cell line demonstrated that endogenous murine *ERFE* and *ENOSF1* did not undergo alternative splicing (12). After transfection, the alternative 3'ss AG' *ERFE*$^{+12}$ was detected by capillary electrophoresis in G1E-ER4 *SF3B1*^{K700E} cells, but not in the isogenic G1E-ER4 *SF3B1*^{WT} or parental cells (Fig. 3B). The usage of alternative 3'ss AG' was detectable for *ENOSF1* gene in *SF3B1*^{WT} cell line and became predominant in *SF3B1*^{K700E} cell line, suggesting that the mutation favored the usage of alternative AG'. Then, we performed a rescue experiment by adding a destabilization domain (DD)-tag to the mutant *SF3B1*^{R625G} allele in Mel202 cell line, as described (31). The DD-tagged protein is stabilized by interaction with the DD ligand Shield-1 and is degraded upon Shield-1 withdrawal. In Mel202 clone 26 containing one DD-tagged *SF3B1*^{R625G} allele, Shield-1 removal abrogated *ERFE*$^{+12}$ expression. This supports a causal relationship between *SF3B1* mutation and the aberrant splicing isoform of *ERFE* (fig. S3).

We then investigated the expression of *ERFE*^{WT} and *ERFE*$^{+12}$ in primary BM samples of MDS patients using fluorescent PCR and RT-qPCR (table S3). Among 46 lower risk MDS patients, *SF3B1*^{MUT} was present in 25, including 20 with MDS-SLD-RS/MDS-MLD-RS, 3 with MDS-MLD, and 2 with MDS-EB1. By fluorescent PCR, *ERFE*$^{+12}$ was detected in the BM MNC fractions of all *SF3B1*^{MUT} MDS. *ERFE*$^{+12}$ was not detected in any other cases of MDS with mutations in *SRSF2* (n=10), *U2AF1* (n=1), or *ZRSR2* (n=1), or in 9 MDS patients with mutations in other genes, as shown in Fig. 3C and table S4. *ERFE*^{WT} and *ERFE*$^{+12}$ mRNA amounts measured by RT-qPCR were up-regulated in *SF3B1*^{MUT} samples compared to any *SF3B1*^{WT} samples with other splicing or epigenetic mutations or without recurrent mutation (Fig. 3D, table S4). In one patient with an *SF3B1* monoallelic deletion and a G742D substitution on the remaining allele, the expression of alternative *ERFE*$^{+12}$ exceeded that of the canonical *ERFE*^{WT} (fig. S4). We then amplified primary erythroblasts from the BM CD34^{+} cells of two patients with *SF3B1*^{MUT} and one patient with *SF3B1*^{WT} MDS and showed that *ERFE*$^{+12}$ was expressed in *SF3B1*^{MUT} but not in *SF3B1*^{WT} erythroid cells (Fig. 3E). This further supports the idea that *ERFE*$^{+12}$ is related to *SF3B1* mutation. *SF3B1*^{MUT} MDS are characterized by the enrichment of the BM with erythroid cells. To investigate whether *ERFE*$^{+12}$ could be detected in cells derived from erythroblastic BM with

another genetic background, we collected samples from one patient with MDS-RS with 38% of BM erythroblasts, more than 15% of RS, a normal karyotype, and no *SF3B1* mutation but one *SRSF2* and one *TET2* mutation, three patients with a congenital sideroblastic anemia due to an *ALAS2* mutation/deletion or a *GLRX5* mutation, one patient with a severe β-thalassemia, and one patient with $SF3B1^{K700E}$ MDS. By fluorescent PCR, $ERFE^{WT}$ was present, whereas $ERFE^{+12}$ was not detectable in any sample except the $SF3B1^{K700E}$ MDS (Fig. 3F). This confirms that the onset of an aberrant $ERFE^{+12}$ is dependent not on the amplification of the erythroid compartment or the presence of RS, but on the presence of a mutant *SF3B1*.

Translation of $ERFE^{+12}$ into a variant protein that represses hepcidin

Human ERFE encodes a 354-aminoacid polypeptide. The addition of 12 nucleotides in *ERFE* mRNA generates an ERFE variant (further referred to as $ERFE^{VPFQ}$) containing a valine-proline-phenylalanine-glutamine (VPFQ) insertion immediately upstream of the collagen domain (Fig. 4A & fig. S5A). To investigate whether the mutant $ERFE^{VPFQ}$ protein was produced in vivo, we prepared cell lysates of erythroblasts derived in culture from the BM $CD34^+$ cells of patients with $SF3B1^{MUT}$ MDS. Through LC MS/MS protein identification, we obtained several peptide-matching propositions including the ALHELGVYYLPDAEGAFR peptide (fig. S5B) already reported in public databases (www.proteomicsdb.org/), and we identified a cryptic peptide VPFQFGLPGPPGPPGPQGPP GPIIPPEALLK corresponding to the VPFQ insertion at position 108 of ERFE (Fig. 4B). This confirms that the alternative $ERFE^{+12}$ transcript is translated into $ERFE^{VPFQ}$ in $SF3B1^{MUT}$ erythroblasts.

ERFE represses hepcidin in mice and contributes to pathological hepcidin suppression in patients with transfused and non-transfused β-thalassemia (28, 29). Whether $ERFE^{VPFQ}$ also repressed hepcidin was tested. For this purpose, recombinant proteins $ERFE^{WT}$ and $ERFE^{VPFQ}$ were produced in HEK293F cells. SDS-PAGE analysis of $ERFE^{WT}$ and $ERFE^{VPFQ}$ in reducing and non-reducing conditions demonstrated that the insertion of 4 amino acids does not change the molecular weight of the protein or its multimerization pattern, such that both proteins were predominantly found in high molecular weight forms (>250 kDa) and in a trimeric form of ~200 kDa (Fig. 4C). Then, Hep3B and HepG2 hepatocellular carcinoma cells were treated for 16h with purified $ERFE^{VPFQ}$ or $ERFE^{WT}$. Both proteins similarly caused a 5-fold reduction in the expression of *HAMP* mRNA encoding hepcidin compared to controls (Fig. 4D). These data indicate that insertion of 4 amino acids upstream of the collagen domain did not affect the bioactivity of the protein.

Prediction of hyperferritinemia by overproduction of erythroferrone in $SF3B1^{MUT}$ MDS

We then measured the plasma concentration of ERFE in the training cohort of 156 patients with MDS and 20 healthy non-blood donor controls using a validated immunoassay (29). We first verified that the ERFE immunoassay was able to detect both $ERFE^{WT}$ and $ERFE^{VPFQ}$. Indeed, human ERFE ELISA detected similar amounts (1 μg/ml) of each recombinant protein in the supernatants of HEK293F cells transiently transfected with $ERFE^{WT}$ and $ERFE^{VPFQ}$ expression vectors. This established that both isoforms were detectable by ELISA. The mean concentration of ERFE in $SF3B1^{MUT}$ or $SF3B1^{WT}$ MDS

was higher than in 20 non-blood donor healthy controls (P<0.0001; Fig. 5A). Among the MDS samples, the ERFE concentration was higher in *SF3B1*^{MUT} (135.0±72.5 ng/ml) compared to *SF3B1*^{WT} (62.1±36.7 ng/ml) MDS (P<0.0001; Fig. 5A). High concentrations of circulating ERFE correlated with high expression of *ERFE*$^{+12}$ transcript (Pearson test; P<0.0001; fig. S6A). Consistently, the ERFE concentration was also higher in MDS-RS compared to all other WHO MDS subtypes (fig. S6B). Ferritin concentrations were significantly higher in *SF3B1*^{MUT} patients compared to *SF3B1*^{WT} patients (P<0.0001; Fig. 5B). We also measured plasma hepcidin and confirmed that the concentration of hepcidin in *SF3B1*^{MUT} MDS was significantly lower compared to *SF3B1*^{WT} MDS (P=0.031; Fig. 5C). We found no difference between *SF3B1*^{MUT} MDS and healthy controls. The hepcidin/ferritin ratio was lower in *SF3B1*^{MUT} than in*SF3B1*^{WT} MDS (P<0.0001; Fig. 5D) and also in MDS-RS compared to other WHO subtypes (fig. S6C), resulting from both a lower concentration of hepcidin and a higher concentration of ferritin in *SF3B1*^{MUT} patients. The plasma concentration of ERFE was inversely correlated to the hepcidin/ferritin ratio (Pearson test; P<0.0001; r=0.600; fig. S6D). Our analysis also highlights that an ERFE concentration above a threshold of 100 ng/ml repressed hepcidin more efficiently (fig. S6D). Serum erythropoietin (EPO) concentration was equally increased in *SF3B1*^{MUT} and *SF3B1*^{WT} patients compared to normal values (5 – 36 U/l; table S1), and although ERFE is regulated by erythropoietin in mice, we did not find any correlation between serum EPO and ERFE concentration (fig. S6E) (28). The increased concentration of plasma ERFE was associated with a more pronounced degree of ineffective erythropoiesis, as assessed by a significant increase in plasma concentration of soluble transferrin receptor (sTfR) in *SF3B1*^{MUT} compared to *SF3B1*^{WT} MDS patients (P<0.0001; fig. S6F).

To validate these findings, we prospectively enrolled an external cohort of lower risk MDS patients in our study until the proportion of patients with *SF3B1*^{MUT} MDS was comparable to that in the training cohort (table S5). This validation cohort consisted of 55 patients with MDS, 42 (76.3%) of whom had MDS with *SF3B1* mutation. Notably, *SF3B1*^{MUT} and *SF3B1*^{WT} patients of this cohort received a similar transfusion burden with a mean number of 4 RBC units/8 weeks (table S5). The mean concentrations of ERFE and ferritin were significantly increased (P=0.0005 and P=0.0488, respectively; Fig. 5E, 5F), whereas hepcidin and hepcidin/ferritin ratio were significantly decreased in *SF3B1*^{MUT} patients (P=0.0038 and P=0.0002, respectively; Fig. 5G, 5H). This confirms the results of the training cohort and suggests that the increase of ERFE concentration in *SF3B1*^{MUT} MDS patients is independent of RBC transfusions.

Iron homeostasis changes after RBC transfusions, which ameliorate the anemia and increase the concentrations of circulating iron, with both effects expected to increase hepcidin. To assess the influence of RBC transfusion in our analysis, we delineated a subset of 61 patients with MDS in the training cohort, including 25 *SF3B1*^{MUT} and 36 *SF3B1*^{WT} patients with a low transfusion burden before inclusion (<4 RBC units per 8 weeks). In this subset, patients with *SF3B1*^{MUT} or *SF3B1*^{WT} MDS were equally transfused (mean 0.5 RBC unit/8 weeks), but ferritin and plasma iron concentrations remained higher in *SF3B1*^{MUT} patients (fig. S7A, S7B). The hepcidin/ferritin and hepcidin/plasma iron ratios were significantly lower in *SF3B1*^{MUT} patients (P<0.0001 and P=0.019, respectively; fig. S7C, S7D), and the circulating ERFE concentration remained significantly increased in low transfusion burden

SF3B1^{MUT} patients compared to *SF3B1*^{WT} patients (P<0.0001; fig. S7E). Erythropoiesis-stimulating agents (ESA) are used as first line treatment of anemia, with low serum EPO and low transfusion burden as predictors of response (25). We investigated the impact of iron parameters on the response to epoetin ζ for 12 weeks in 59 patients with low-risk MDS included in a clinical trial of the Groupe Francophone des Myélodysplasies (GFM), GFM-Retacrit-2013 (NCT 03598582; table S6) (32). Plasma ERFE, ferritin, and hepcidin concentrations at enrollment were similar in responding and non-responding patients, suggesting that these parameters were not predictive of the erythropoietic response in this cohort (fig. S8). We then explored the determinants of hyperferritinemia >300 μg/ml in low transfusion burden patients. By univariate analysis, ERFE (P=0.005), hepcidin (P=0.013), and *SF3B1* mutation (P=0.006), but not sTfR concentration or the number of transfused RBC units, were significantly linked to the concentration of serum ferritin (Table 1). By multivariate analysis, ERFE, hepcidin, and *SF3B1* mutation remained independent predictors of high ferritin concentration (Table 1). Altogether, these results indicate that before patients reach a critical threshold of transfusion dependence, hyperferritinemia can be caused by *SF3B1*^{MUT}-induced expression of ERFE, which in turn lowers hepcidin.

Erythroid lineage-restricted expression of ERFE^{+12}

In mice, *ERFE* mRNA expression in the BM is regulated by EPO and is predominant in basophilic and polychromatic erythroblasts (28). To investigate whether *ERFE* and *ERFE*$^{+12}$ expression is restricted to the erythroid lineage, we amplified in parallel the erythroid and granulocytic precursors derived from the BM CD34^{+} cells of 1 *SF3B1*^{MUT} and 1 *SF3B1*^{WT} sample. The purity of each lineage was assessed by the cytological examination of May-Grünwald-Giemsa-stained cytospins and the quantification of lineage-restricted markers by RT-qPCR (Fig. 6A & fig. S9A). To compare the amount of each transcript isoform at the different stages of differentiation, we quantified the canonical *ERFE*^{WT} and the aberrant *ERFE*$^{+12}$ by RT-qPCR. The expression of the canonical transcript *ERFE*^{WT} expressed as Normalized Ratio Quantities (NRQ) increased in both *SF3B1*^{MUT} and *SF3B1*^{WT} MDS erythroblasts. In granulocytes, the expression of *ERFE*^{WT} was close to the limit of detection (Fig. 6B). The expression of *ERFE*$^{+12}$ was restricted to the erythroid lineage, increased with the differentiation of *SF3B1*^{MUT} erythroblasts, and was higher in *SF3B1*^{MUT} compared to *SF3B1*^{WT} erythroblasts (Fig. 6B). These results indicate that *ERFE*$^{+12}$ expression is specific to the erythroid lineage.

SF3B1 gene is mutated in 15% of patients suffering from CLL and the *SF3B1*^{MUT} allele is present in CD19^{+} lymphocytes (14, 33). To investigate whether *ERFE*$^{+12}$ was detectable in *SF3B1*^{MUT} CLL, we collected one sample from a patient with CLL followed by MDS, whose BM MNC expressed a clonal *SF3B1*^{K700E} mutation, and 3 peripheral blood (PB) MNC samples from 2 patients with CLL, one of whom harbored a clonal *SF3B1*^{T663I} mutation with a variant allele frequency over 40% and the second had no mutation in *SF3B1* gene, and from a patient with *SF3B1*^{K700E} MDS. We analyzed the *MAP3K7* transcript, which is alternatively spliced in *SF3B1*^{MUT} CLL or MDS using a cryptic 3'ss (14, 16). A 170 nt fragment corresponding to the alternative *MAP3K7* transcript was enriched in all *SF3B1*^{MUT} samples compared to the *SF3B1*^{WT} CLL (Fig. 6C). *ERFE*$^{+12}$ was detected in the PB MNC of the *SF3B1*^{K700E} MDS, but not in the *SF3B1*^{T663I} or *SF3B1*^{WT} CLL. *ERFE*$^{+12}$

was not detected in BM MNC of the *SF3B1*^{K700E} CLL+MDS sample. To get further insights on the cell types expressing *ERFE*$^{+12}$, we sorted CD19^{+}CD5^{-} B cells, CD19^{+}CD5^{+} pathological B cells, and CD3^{+} T cells and myeloid cells containing erythroblasts from the BM MNC fraction of the patients with *SF3B1*^{K700E} CLL+MDS, *SF3B1*^{K700E} MDS, and *SF3B1*^{WT} MDS and from the PB MNC of the patient with *SF3B1*^{T663I} CLL (fig. S9B). The number of cells in the myeloid fraction of *SF3B1*^{T663I} CLL was too small for further studies. The 170 nt fragment of *MAP3K7* was detected in CD19^{+}CD5^{+} pathological B cells of *SF3B1*^{K700E} CLL+MDS and *SF3B1*^{T663I} CLL and also in the myeloid fraction, but not in the CD19^{+}CD5^{-} B cells of *SF3B1*^{K700E} MDS (Fig. 6D). By sequencing *SF3B1* RNA, we demonstrated that the mutation was present in the cell populations in which the alternative *MAP3K7* transcript was detected (Fig. 6E). The alternative *ERFE*$^{+12}$ transcript was not detected in the CD19^{+}CD5^{+} pathological B cells of *SF3B1*^{K700E} MDS+CLL or *SF3B1*^{T663I} CLL, and its expression was restricted to *SF3B1*^{K700E} myeloid MDS cells. Altogether, these results indicate that *ERFE* is expressed in erythroid cells and *ERFE*$^{+12}$ is restricted to *SF3B1*^{MUT} MDS myeloid cells.

Correlation between changes in ERFE^{+12} expression and the response to lenalidomide

Fifty percent of lower risk MDS patients, including patients with MDS-RS, experience primary resistance or secondary failure to treatments they receive to cure their anemia. Whether the mechanism of resistance involves the persistence of clonal erythropoiesis is always unknown. We have previously shown that lenalidomide administered to ESA-resistant non-del(5q) MDS patients targets the malignant clone and in some cases, eliminates the dominant *SF3B1*^{MUT} clone for the duration of response (34). However, the frequency of the *SF3B1* variant allele, which is expressed in erythroid and myeloid cells, does not only reflect the abundance of clonal erythroblasts. Here, we retrospectively monitored the expression of erythroid-specific *ERFE*$^{+12}$ transcript for the follow-up of patients included in clinical trials of the GFM: GFM-Retacrit-2013 and GFM-LenEpo-2008 ((32,35). For this purpose, we performed a fluorescent PCR and integrated *ERFE*$^{+12}$ and *ERFE*^{WT} peak heights as a ratio *ERFE*$^{+12}$/*ERFE*$^{+12}$+*ERFE*^{WT} in *SF3B1*^{MUT} MDS patients. Then, the ratio was measured in paired RNA samples at enrollment and first evaluation. In GFM-Retacrit-2013, 4 non-responders and 6 responders were compared, and no significant variation was observed (Fig. 7A, fig. S10A). By contrast, in GFM-LenEpo-2008, the ratio *ERFE*$^{+12}$/*ERFE*$^{+12}$+*ERFE*^{WT} decreased in 6 responding patients but remained stable in 8 non-responding patients (Fig. 7B, fig. S10B). The percent variation of ratios between samples obtained during screening and after 4 cycles of treatment was significantly different between responding and non-responding patients (Mann-Whitney test P=0.0013; Fig. 7B, **right**). The percent variation of *SF3B1* variant allele frequency in BM mononuclear cells between screening and evaluation after 4 cycles was not significantly different between non-responding and responding patients (fig. S10C). This confirms that lenalidomide may target clonal erythropoiesis. By contrast, ERFE protein quantities did not vary with the response in both cohorts (fig. S11). Finally, we addressed the prognostic value of the *ERFE*$^{+12}$/*ERFE*$^{+12}$+*ERFE*^{WT} ratio for overall survival (OS) in a cohort of 90 patients with low-risk MDS, including 24 patients with *SF3B1*^{MUT} and 66 with *SF3B1*^{WT} enrolled at diagnosis with a median follow-up of 36.9 months (table S7). In this cohort, a Receiver Operating Characteristic (ROC) analysis established that a value of 0.008 was the threshold of

positivity of the $ERFE^{+12}/ERFE^{+12}+ERFE^{WT}$ ratio with a specificity and sensitivity of 100%. As shown in Fig. 7C, an $ERFE^{+12}/ERFE^{+12}+ERFE^{WT}$ ratio >0.008, was predictive of better OS (log-rank test; P=0.019) and was correlated with the presence of an *SF3B1* mutation Among patients expressing the variant $ERFE^{+12}$ transcript, there was no significant correlation between $ERFE^{+12}/ERFE^{+12}+ERFE^{WT}$ ratio and OS (log-rank test; P=0.064; fig. S12). Our results suggest that $ERFE^{+12}$ expression may correlate with OS for $SF3B1^{MUT}$ MDS patients.

Discussion

In this study, we show that in patients with $SF3B1^{MUT}$ MDS, an alternative *FAM132B/* $ERFE^{+12}$ transcript is translated into an $ERFE^{VPFQ}$ protein and, together with the canonical transcript, contributes to the overexpression of ERFE. Similarly to ERFE, the $ERFE^{VPFQ}$ protein efficiently represses hepcidin. $ERFE^{+12}$ is specifically induced by the clonal erythropoiesis.

In $SF3B1^{MUT}$ cancers, alternative 3'ss usages are the most frequent splicing aberrancies (11, 13, 14, 36). The recently resolved crystal structure of SF3b complex helps understanding this feature (37). In the spliceosome, SF3b complex interacts with the pre-mRNA and is involved in the branch site selection during splicing. Mutations in *SF3B1* affect the structure of SF3b RNA-binding platform, resulting in the selection of alternative branch site and alternative transcripts, of which more than 50% are subjected to NMD (11, 13, 37). Based on these findings, we focused our attention on the transcripts generated by the use of an alternative AG'. The analysis of the distance separating AG from AG' revealed strong peaks at 15, 18, and 21 nucleotides, showing that inserts could be multiples of 3 nucleotides. Among alternative in-frame junctions, we identified two regulators of iron homeostasis, *ABCB7* and *ERFE*. As already reported, the alternative *ABCB7* mRNA results from the addition of 21 nucleotides between exon 8 and 9 and, in our sample set, was slightly down-regulated in $SF3B1^{MUT}$ compared to $SF3B1^{WT}$ MDS (11, 15, 16). By contrast, the aberrant *ERFE* transcript modified by the addition of 12 nucleotides was up-regulated 2.3 fold in $SF3B1^{MUT}$ MDS. $ERFE^{+12}$ has not been reported in other $SF3B1^{MUT}$ cancers despite some overlap between the sets of alternative 3'ss transcripts in $SF3B1^{MUT}$ uveal melanoma, CLL, and MDS (11, 13, 14, 38, 39). We showed the existence of a variant protein containing VPFQ sequence immediately upstream of the collagen domain putatively involved in protein-protein interactions in other CTRP family members (40). VPFQ may not influence protein conformation, because the apparent molecular weight was similar for recombinant $ERFE^{WT}$ and $ERFE^{VPFQ}$ proteins, which both repressed *HAMP* gene expression. However, we could not exclude an effect of the VPFQ insertion on protein stability and/or still unknown functions.

In MDS, serum EPO is increased but ineffective in stimulating erythropoiesis because maturing erythroid cells undergo apoptosis in terminal phases of differentiation (1, 2). Increased EPO and sTfR concentrations have been inversely correlated with hepcidin concentrations in MDS (19, 20, 41, 42). Our study indicates that plasma hepcidin concentration in $SF3B1^{MUT}$ MDS is similar to healthy non-blood donor controls and inappropriately low compared to $SF3B1^{WT}$ MDS, suggesting that its production could be

dysregulated by severe ineffective erythropoiesis and/or a more specific mechanism (19). We showed the cell-autonomous *SF3B1*^{MUT}-dependent expression of *ERFE*$^{+12}$ and a role for increased concentrations of circulating ERFE in hepcidin reduction. This confirms the involvement of ERFE in human pathologies (29).

ERFE is the major erythroid regulator of hepcidin (28). Other candidate regulators of hepcidin linked to erythropoiesis have been proposed, including EPO and GDF-15. Although EPO administration decreases hepcidin concentration (43), this effect is predominantly indirect. The other candidate, GDF-15, is poorly induced by EPO in human volunteers. Although serum GDF-15 concentration was increased in β-thalassemia or congenital dyserythropoietic anemia, it was not inversely correlated with hepcidin in MDS (19, 26, 44). Low hepcidin preserves ferroportin on enterocytes and macrophages, causing increased iron intestinal absorption and macrophage release (45, 46). Compared to *SF3B1*^{WT} MDS, the lower concentrations of hepcidin in *SF3B1*^{MUT} MDS may explain early iron overload, before patients receive erythrocyte transfusions (19, 20). In patients with low transfusion burden, who had received a mean of 0.5 RBC unit, hepcidin, ERFE and *SF3B1* mutation were independent predictors of hyperferritinemia. This demonstrates that iron overload is strongly related to the control of hepcidin through the *SF3B1*-regulated production of ERFE. Hepcidin increases with transfusion intensity in patients with MDS or β-thalassemia because of exogenous iron loading and transient suppression of ineffective erythropoiesis (29, 47, 48). Here, in regularly transfused *SF3B1*^{MUT} MDS patients, hepcidin remained lower and ERFE higher than in *SF3B1*^{WT} MDS patients. This establishes a driver role for *SF3B1* mutation in the stimulation of ERFE expression and systemic iron overload that characterized patients.

The *SF3B1* mutation confers a good prognosis in MDS (6, 49). However, when patients are transfusion-dependent, iron overload in cardiac and liver tissues becomes clinically evident and may impair life expectancy (50). Chelation efficiently reduces iron burden in regularly transfused MDS patients and serves as an adjuvant therapy for anemia, because deferasirox may improve hematopoiesis by protecting against oxidative stress (51–53). Promising substitutes for ESAs in resistant patients include lenalidomide, which may transiently reduce *SF3B1* mutant allele burden, and activin receptor ligand traps such as luspatercept, which promotes late-stage erythropoiesis in mouse models of β-thalassemia and MDS and diminishes iron overload in β-thalassemia mice (34, 54–56). In lenalidomide-treated patients, but not in epoetin ζ-treated patients, the kinetics of *ERFE*$^{+12}$ expression correlated with the response to treatment, indicating that in responding patients lenalidomide targeted clonal erythroid precursors either directly or indirectly. Of note, changes in plasma ERFE protein after lenalidomide were not correlated with the response to these treatments. The impact of transfusions on the regulation of ERFE expression at the post-transcriptional level should be examined in the future. *ERFE*$^{+12}$ expression could also be useful for disease surveillance of patients with MDS-RS treated with other drugs, such as luspatercept. Further clinical studies will be required to validate *ERFE*$^{+12}$ expression as a therapy-responsive biomarker of ineffective erythropoiesis in patients with *SF3B1*^{MUT} MDS.

Finally, our findings open therapeutic avenues for preventing iron accumulation in MDS-RS patients. Increasing hepcidin could produce therapeutic benefits in *SF3B1*^{MUT} MDS,

because a moderate increase in hepcidin decreased iron and improved anemia in β-thalassemia mice (57). Therefore, either the administration of a hepcidin agonist or the targeting of erythroferrone overexpression may provide a potential strategy for preventing iron overload and improving erythropoiesis in *SF3B1*^{MUT} MDS patients.

Materials and Methods

Study design

The study involved identifying a splicing variant of *ERFE* by RNA-sequencing human primary BM samples and the variant peptide by mass spectrometry. Each in vitro experiments transfection, minigene assay, degron-KI, transcriptional repression of hepcidin was repeated three times. Each experiment using primary cells was performed with at least three samples in each category. A ratio of *ERFE* variant transcript to total transcript was validated as a marker of clonal erythropoiesis based on the response to lenalidomide or ESA in two cohorts of MDS patients enrolled in clinical trials and as a prognostic marker of overall survival in a prospective multicenter cohort of MDS patients. Predictive value of plasma erythroferrone and hepcidin concentrations for hyperferritinemia was measured in training and validation cohorts of MDS patients. For these studies, randomization or blinding were not applicable

Patients

For the training cohort, MDS patients (n=156) were enrolled between 2008 and 2017 (ClinicalTrials.gov: GFM-LenEpo-2008, NCT01718379; GFM-Retacrit-2013, NCT 03598582). For the GFM-Retacrit-2013 cohort, the status of response to epoetin ζ was recorded. The prospective cohort of 90 MDS patients with survival data was enrolled between 2010 and 2018. BM aspirates and PB plasma samples were collected after each patient gave informed consent for biological investigations according to the recommendations of the institutional review boards (IRB): IdF X GFM-LenEpo-08 EudraCT 2008-008262-12; IdFII 2010-A00033-36; IdFIII: 2010-2753; IdFV 212-A01395-38 EudraCT 2012-002990-7338; OncoCCH 2015-08-11-DC). For the validation cohort, MDS patients (n=55) were enrolled prospectively for plasma collection in France (5 centers; IRB Onco-CCH 2015-08-11DC) and Germany (one center; IRB Ethikkommission an der TU Dresden; EK 115032015) between 2016 and 2018. BM samples from 5 age-matched controls and PB plasma samples from 20 healthy controls were collected. Patient characteristics are indicated in tables S1, S5, and S7 and according to the response to epoetin ζ in table S6. Low transfusion burden was defined as <4 RBC units per 8 weeks.

DNA and RNA-sequencing

Mutations in a panel of 26 genes were screened by next-generation sequencing (NGS) (fig. S1). RNA was sequenced on an Illumina HiSeq 2500 platform using a 100-bp paired-end sequencing strategy. TopHat (v2.0.6) was used to align the reads against the human reference genome Hg19 RefSeq (RNA sequences, GRCh37) downloaded from the UCSC Genome Browser (http://genome.ucsc.edu). Analyses of differential gene expression analysis and differential junction read counts were performed using DESeq2 (13, 30).

CRISPR/Cas9 generation of isogenic Sf3b1^{K700E} and Sf3b1^{WT} cell lines

The murine erythroid cell line G1E-ER4 (58) was used to generate isogenic *Sf3b1*^{K700E} and *Sf3b1*^{WT} cell lines using CRISPR/Cas9-stimulated homology-mediated repair.

ERFE and ENOSF1 minigenes

The *ERFE* minigene was synthesized by insertion of the *ERFE* alternative junction in pET01 Exontrap vector (Mobitec). G1E-ER4 9.2 (*SF3B1*^{WT}) and G1E-ER4 5.13H (*SF3B1*^{K700E}) cells were transfected and processed for fluorescent PCR.

Mass spectrometry analysis

Erythroblasts were lysed and peptides were obtained by trypsin digestion (Promega) and analyzed by nano liquid chromatography coupled with a Q-Exactive Plus mass spectrometer (Thermo). Data were analyzed using Mascot 2.5.1 (www.matrixscience.com).

Human erythroferrone quantification

Plasma erythroferrone concentration was determined as previously described (29).

Statistical analysis

For quantitative variables, values were compared using the Mann-Whitney test. Categorical variables were compared using X^2 or Fisher's exact tests. *P*-values<0.05 were considered significant. Receiver operating characteristic (ROC) analysis was used to calculate the thresholds of positivity. Multivariate logistic regression analysis was adjusted for selected variables chosen with a *P*-value<0.1 in univariate analysis (JMP version 10.0.2, SAS Institute Inc.).

Supplementary Material

Refer to Web version on PubMed Central for supplementary material.

Acknowledgements

The authors want to thank Dr F. Pflumio (INSERM UMR967, CEA/DSV/iRCM, Fontenay-aux-Roses), Dr N. Taylor (Institut de Génétique Moléculaire, Montpellier) and Dr S. Vaulont (Institut Cochin), Dr E-F Gautier (3P5 proteomic platform), Dr J. Vinh (Ecole Supérieure de Physique et de Chimie Industrielles, Paris), B. Saint-Pierre (Institut Cochin) and D. Drubay (Institut Gustave Roussy) for fruitful discussions; Dr J-B Arlet, Service de Médecine Interne, Hôpital Européen Pompidou, Dr C. Kannengiesser, Service de Génétique, Hôpital Bichat, for providing samples; Dr F. Letourneur (Genom'IC, Institut Cochin), Dr S. Baulande (sequencing platform, Institut Curie), L. Zaroili, M. Dejean, A. Marcon, V. Verjus-Lisfranc (Cochin laboratory of hematology), E. Benana (3P5 platform) and B. Billoré (INSERM U1220) for technical assistance, Pr M. Weiss, St Jude Children's research hospital (Memphis, TN) and Dr V. Paralkar, University of Pennsylvania (Philadelphia, PA) for providing the G1E-ER4 cell line and expert comments.

Funding: This study was funded by INSERM, by the Institut National du Cancer INCa PLBio 2015 (INCa_9290), by INCa and the Direction Générale de l'Offre de Soins (DGOS) of the French Ministry of Social Affairs and Health through the Programme Hospitalier de Recherche Clinique (PHRC MDS-04; INCa-DGOS_5480) and by the Site de Recherche Intégrée sur le Cancer (SIRIC) CAncer Research for PErsonalized Medicine CARPEM. CL and DR are the recipients of a salary funded by the Laboratory of Excellence on red cells GR-Ex. The Orbitrap Fusion MS was acquired with funds from the FEDER and "Canceropole Ile de France". LK received a support from ANR-16-ACHN-0002-01 and from the European Research Council (ERC) under the European Union's Horizon 2020 research and innovation program (Grant agreement N0 715491). TG received funding from NIH by R01 DK 065029 (and the UCLA Center for Accelerated Innovation, under NIH grant U54HL119893 (Palazzolo).

References and notes

1. Tehranchi R, Invernizzi R, Grandien A, Zhivotovsky B, Fadeel B, Forsblom A-M, Travaglino E, Samuelsson J, Hast R, Nilsson L, Cazzola M, Wibom R, Hellström-Lindberg E, Aberrant mitochondrial iron distribution and maturation arrest characterize early erythroid precursors in low-risk myelodysplastic syndromes, Blood 106, 247–253 (2005). [PubMed: 15755901]
2. Gyan E, Frisan E, Beyne-Rauzy O, Deschemin J-C, Pierre-Eugene C, Randriamampita C, Dubart-Kupperschmitt A, Garrido C, Dreyfus F, Mayeux P, Lacombe C, Solary E, Fontenay M, Spontaneous and Fas-induced apoptosis of low-grade MDS erythroid precursors involves the endoplasmic reticulum, Leukemia 22, 1864–1873 (2008). [PubMed: 18615109]
3. Zhu Y, Li X, Chang C, Xu F, He Q, Guo J, Tao Y, Liu Y, Liu L, Shi W, SF3B1-mutated myelodysplastic syndrome with ring sideroblasts harbors more severe iron overload and corresponding over-erythropoiesis, Leukemia Research 44, 8–16 (2016). [PubMed: 26970172]
4. de Swart L, Reiniers C, Bagguley T, van Marrewijk C, Bowen D, Hellström-Lindberg E, Tatic A, Symeonidis A, Huls G, Cermak J, van de Loosdrecht AA, Garelius H, Culligan D, Macheta M, Spanoudakis M, Panagiotidis P, Krejci M, Blijlevens N, Langemeijer S, Droste J, Swinkels DW, Smith A, de Witte T, Labile plasma iron levels predict survival in patients with lower-risk myelodysplastic syndromes, Haematologica 103, 69–79 (2018). [PubMed: 29122992]
5. Yoshida K, Sanada M, Shiraishi Y, Nowak D, Nagata Y, Yamamoto R, Sato Y, Sato-Otsubo A, Kon A, Nagasaki M, Chalkidis G, Suzuki Y, Shiosaka M, Kawahata R, Yamaguchi T, Otsu M, Obara N, Sakata-Yanagimoto M, Ishiyama K, Mori H, Nolte F, Hofmann W-K, Miyawaki S, Sugano S, Haferlach C, Koeffler HP, Shih L-Y, Haferlach T, Chiba S, Nakauchi H, Miyano S, Ogawa S, Frequent pathway mutations of splicing machinery in myelodysplasia, Nature 478, 64–69 (2011). [PubMed: 21909114]
6. Papaemmanuil E, Cazzola M, Boultwood J, Malcovati L, Vyas P, Bowen D, Pellagatti A, Wainscoat JS, Hellstrom-Lindberg E, Gambacorti-Passerini C, Godfrey AL, Rapado I, Cvejic A, Rance R, McGee C, Ellis P, Mudie LJ, Stephens PJ, McLaren S, Massie CE, Tarpey PS, Varela I, Nik-Zainal S, Davies HR, Shlien A, Jones D, Raine K, Hinton J, Butler AP, Teague JW, Baxter EJ, Score J, Galli A, Della Porta MG, Travaglino E, Groves M, Tauro S, Munshi NC, Anderson KC, El-Naggar A, Fischer A, Mustonen V, Warren AJ, Cross NCP, Green AR, Futreal PA, Stratton MR, Campbell PJ, Chronic Myeloid Disorders Working Group of the International Cancer Genome Consortium, Somatic SF3B1 mutation in myelodysplasia with ring sideroblasts, N. Engl. J. Med 365, 1384–1395 (2011). [PubMed: 21995386]
7. Damm F, Kosmider O, Gelsi-Boyer V, Renneville A, Carbuccia N, Hidalgo-Curtis C, Della Valle V, Couronné L, Scourzic L, Chesnais V, Guerci-Bresler A, Slama B, Beyne-Rauzy O, Schmidt-Tanguy A, Stamatoullas-Bastard A, Dreyfus F, Prébet T, de Botton S, Vey N, Morgan MA, Cross NCP, Preudhomme C, Birnbaum D, Bernard OA, Fontenay M, Groupe Francophone des Myélodysplasies, Mutations affecting mRNA splicing define distinct clinical phenotypes and correlate with patient outcome in myelodysplastic syndromes, Blood 119, 3211–3218 (2012). [PubMed: 22343920]
8. Mian SA, Rouault-Pierre K, Smith AE, Seidl T, Pizzitola I, Kizilors A, Kulasekararaj AG, Bonnet D, Mufti GJ, SF3B1 mutant MDS-initiating cells may arise from the haematopoietic stem cell compartment, Nature Communications 6, 10004 (2015).
9. Chesnais V, Arcangeli M-L, Delette C, Rousseau A, Guermouche H, Lefevre C, Bondu S, Diop M, Cheok M, Chapuis N, Legros L, Raynaud S, Willems L, Bouscary D, Lauret E, Bernard OA, Kosmider O, Pflumio F, Fontenay M, Architectural and functional heterogeneity of hematopoietic stem/progenitor cells in non-del(5q) myelodysplastic syndromes, Blood 129, 484–496 (2017). [PubMed: 27856460]
10. Mortera-Blanco T, Dimitriou M, Woll PS, Karimi M, Elvarsdottir E, Conte S, Tobiasson M, Jansson M, Douagi I, Moarii M, Saft L, Papaemmanuil E, Jacobsen SEW, Hellström-Lindberg E, SF3B1-initiating mutations in MDS-RSs target lymphomyeloid hematopoietic stem cells, Blood 130, 881–890 (2017). [PubMed: 28634182]
11. Darman RB, Seiler M, Agrawal AA, Lim KH, Peng S, Aird D, Bailey SL, Bhavsar EB, Chan B, Colla S, Corson L, Feala J, Fekkes P, Ichikawa K, Keaney GF, Lee L, Kumar P, Kunii K, MacKenzie C, Matijevic M, Mizui Y, Myint K, Park ES, Puyang X, Selvaraj A, Thomas MP, Tsai

J, Wang JY, Warmuth M, Yang H, Zhu P, Garcia-Manero G, Furman RR, Yu L, Smith PG, Buonamici S, Cancer-Associated SF3B1 Hotspot Mutations Induce Cryptic 3' Splice Site Selection through Use of a Different Branch Point, Cell Rep 13, 1033–1045 (2015). [PubMed: 26565915]

12. Obeng EA, Chappell RJ, Seiler M, Chen MC, Campagna DR, Schmidt PJ, Schneider RK, Lord AM, Wang L, Gambe RG, McConkey ME, Ali AM, Raza A, Yu L, Buonamici S, Smith PG, Mullally A, Wu CJ, Fleming MD, Ebert BL, Physiologic Expression of Sf3b1(K700E) Causes Impaired Erythropoiesis, Aberrant Splicing, and Sensitivity to Therapeutic Spliceosome Modulation, Cancer Cell 30, 404–417 (2016). [PubMed: 27622333]
13. Alsafadi S, Houy A, Battistella A, Popova T, Wassef M, Henry E, Tirode F, Constantinou A, Piperno-Neumann S, Roman-Roman S, Dutertre M, Stern M-H, Cancer-associated SF3B1 mutations affect alternative splicing by promoting alternative branchpoint usage, Nat Commun 7, 10615 (2016). [PubMed: 26842708]
14. Wang L, Brooks AN, Fan J, Wan Y, Gambe R, Li S, Hergert S, Yin S, Freeman SS, Levin JZ, Fan L, Seiler M, Buonamici S, Smith PG, Chau KF, Cibulskis CL, Zhang W, Rassenti LZ, Ghia EM, Kipps TJ, Fernandes S, Bloch DB, Kotliar D, Landau DA, Shukla SA, Aster JC, Reed R, DeLuca DS, Brown JR, Neuberg D, Getz G, Livak KJ, Meyerson MM, Kharchenko PV, Wu CJ, Transcriptomic Characterization of SF3B1 Mutation Reveals Its Pleiotropic Effects in Chronic Lymphocytic Leukemia, Cancer Cell 30, 750–763 (2016). [PubMed: 27818134]
15. Nikpour M, Scharenberg C, Liu A, Conte S, Karimi M, Mortera-Blanco T, Giai V, Fernandez-Mercado M, Papaemmanuil E, Högstrand K, Jansson M, Vedin I, Stephen Wainscoat J, Campbell P, Cazzola M, Boultwood J, Grandien A, Hellström-Lindberg E, The transporter ABCB7 is a mediator of the phenotype of acquired refractory anemia with ring sideroblasts, Leukemia 27, 889–896 (2013). [PubMed: 23070040]
16. Dolatshad H, Pellagatti A, Liberante FG, Llorian M, Repapi E, Steeples V, Roy S, Scifo L, Armstrong RN, Shaw J, Yip BH, Killick S, Kušec R, Taylor S, Mills KI, Savage KI, Smith CWJ, Boultwood J, Cryptic splicing events in the iron transporter ABCB7 and other key target genes in SF3B1-mutant myelodysplastic syndromes, Leukemia 30, 2322–2331 (2016). [PubMed: 27211273]
17. Pellagatti A, Armstrong RN, Steeples V, Sharma E, Repapi E, Singh S, Sanchi A, Radujkovic A, Horn P, Dolatshad H, Roy S, Broxholme J, Lockstone H, Taylor S, Giagounidis A, Vyas P, Schuh A, Hamblin A, Papaemmanuil E, Killick S, Malcovati L, Hennrich ML, Gavin AC, Ho AD, Luft T, Hellström-Lindberg E, Cazzola M, Smith CWJ, Smith S, Boultwood J. Blood 132, 1225–1240 (2018). [PubMed: 29930011]
18. Shiozawa Y, Malcovati L, Gallì A, Sato-Otsubo A, Kataoka K, Sato Y, Watatani Y, Suzuki H, Yoshizato T, Yoshida K, Sanada M, Makishima H, Shiraishi Y, Chiba K, Hellström-Lindberg E, Miyano S, Ogawa S, Cazzola M. Aberrant splicing and defective mRNA production induced by somatic spliceosome mutations in myelodysplasia. Nat Commun 9, 3649 (2018). [PubMed: 30194306]
19. Santini V, Girelli D, Sanna A, Martinelli N, Duca L, Campostrini N, Cortelezzi A, Corbella M, Bosi A, Reda G, Olivieri O, Cappellini MD, Hepcidin Levels and Their Determinants in Different Types of Myelodysplastic Syndromes, PLOS ONE 6, e23109 (2011). [PubMed: 21886780]
20. Ambaglio I, Malcovati L, Papaemmanuil E, Laarakkers CM, Porta MGD, Gallì A, Già MCD, Bono E, Ubezio M, Travaglino E, Albertini R, Campbell PJ, Swinkels DW, Cazzola M, Inappropriately low hepcidin levels in patients with myelodysplastic syndrome carrying a somatic mutation of SF3B1, Haematologica 98, 420–423 (2013). [PubMed: 23300182]
21. Weinstein DA, Roy CN, Fleming MD, Loda MF, Wolfsdorf JI, Andrews NC, Inappropriate expression of hepcidin is associated with iron refractory anemia: implications for the anemia of chronic disease, Blood 100, 3776–3781 (2002). [PubMed: 12393428]
22. Nicolas G, Chauvet C, Viatte L, Danan JL, Bigard X, Devaux I, Beaumont C, Kahn A, Vaulont S, The gene encoding the iron regulatory peptide hepcidin is regulated by anemia, hypoxia, and inflammation, J Clin Invest 110, 1037–1044 (2002). [PubMed: 12370282]
23. Nemeth E, Valore EV, Territo M, Schiller G, Lichtenstein A, Ganz T, Hepcidin, a putative mediator of anemia of inflammation, is a type II acute-phase protein, Blood 101, 2461–2463 (2003). [PubMed: 12433676]

24. Pak M, Lopez MA, Gabayan V, Ganz T, Rivera S, Suppression of hepcidin during anemia requires erythropoietic activity, Blood 108, 3730–3735 (2006). [PubMed: 16882706]
25. Malcovati L, Papaemmanuil E, Bowen DT, Boultwood J, Porta MGD, Pascutto C, Travaglino E, Groves MJ, Godfrey AL, Ambaglio I, Gallì A, Già MCD, Conte S, Tauro S, Keenan N, Hyslop A, Hinton J, Mudie LJ, Wainscoat JS, Futreal PA, Stratton MR, Campbell PJ, Hellström-Lindberg E, Cazzola M, on behalf of the C. M. D. W. G. of the I. C. G. C. and of the A. I. per la R. sul C. G. I. M. Mieloproliferative, Clinical significance of SF3B1 mutations in myelodysplastic syndromes and myelodysplastic/myeloproliferative neoplasms, Blood 118, 6239–6246 (2011). [PubMed: 21998214]
26. Tanno T, Bhanu NV, Oneal PA, Goh S-H, Staker P, Lee YT, Moroney JW, Reed CH, Luban NL, Wang R-H, Eling TE, Childs R, Ganz T, Leitman SF, Fucharoen S, Miller JL, High levels of GDF15 in thalassemia suppress expression of the iron regulatory protein hepcidin, Nature Medicine 13, 1096–1101 (2007).
27. Tanno T, Porayette P, Sripichai O, Noh S-J, Byrnes C, Bhupatiraju A, Lee YT, Goodnough JB, Harandi O, Ganz T, Paulson RF, Miller JL, Identification of TWSG1 as a second novel erythroid regulator of hepcidin expression in murine and human cells, Blood 114, 181–186 (2009). [PubMed: 19414861]
28. Kautz L, Jung G, Valore EV, Rivella S, Nemeth E, Ganz T, Identification of erythroferrone as an erythroid regulator of iron metabolism, Nature Genetics 46, 678–684 (2014). [PubMed: 24880340]
29. Ganz T, Jung G, Naeim A, Ginzburg Y, Pakbaz Z, Walter PB, Kautz L, Nemeth E, Immunoassay for human serum erythroferrone, Blood 130, 1243–1246 (2017). [PubMed: 28739636]
30. Love MI, Huber W, Anders S, Moderated estimation of fold change and dispersion for RNA-seq data with DESeq2, Genome Biology 15, 550 (2014). [PubMed: 25516281]
31. Zhou Q, Derti A, Ruddy D, Rakiec D, Kao I, Lira M, Gibaja V, Chan H, Yang Y, Min J, Schlabach MR, Stegmeier F, A chemical genetics approach for the functional assessment of novel cancer genes. Cancer Res 75, 1949–1958 (2015). [PubMed: 25788694]
32. Park S, Kosmider O, Maloisel F, Drenou B, Chapuis N, Lefebvre T, Karim Z, Puy H, Alary AS, Ducamp S, Verdier F, Bouilloux C, Rousseau A, Jacob MC, Debliquis A, Charpentier A, Gyan E, Anglaret B, Leyronnas C, Corm S, Slama B, Cheze S, Laribi K, Amé S, Rose C, Lachenal F, Toma A, Pica GM, Carre M, Garban F, Mariette C, Cahn JY, Meunier M, Herault O, Fenaux P, Wagner-Ballon O, Bardet V, Dreyfus F, Fontenay M, Dyserythropoiesis evaluated by the RED score and hepcidin:ferritin ratio predicts response to erythropoietin in lower-risk myelodysplastic syndromes. Haematologica 104, 497–504 (2019). [PubMed: 30287621]
33. Damm F, Mylonas E, Cosson A, Yoshida K, Valle VD, Mouly E, Diop M, Scourzic L, Shiraishi Y, Chiba K, Tanaka H, Miyano S, Kikushige Y, Davi F, Lambert J, Gautheret D, Merle-Béral H, Sutton L, Dessen P, Solary E, Akashi K, Vainchenker W, Mercher T, Droin N, Ogawa S, Nguyen-Khac F, Bernard OA, Acquired Initiating Mutations in Early Hematopoietic Cells of CLL Patients, Cancer Discov 4, 1088–1101 (2014). [PubMed: 24920063]
34. Chesnais V, Renneville A, Toma A, Lambert J, Passet M, Dumont F, Chevret S, Lejeune J, Raimbault A, Stamatoullas A, Rose C, Beyne-Rauzy O, Delaunay J, Solary E, Fenaux P, Dreyfus F, Preudhomme C, Kosmider O, Fontenay M, Effect of lenalidomide treatment on clonal architecture of myelodysplastic syndromes without 5q deletion, Blood 127, 749–760 (2016). [PubMed: 26626993]
35. Toma A, Kosmider O, Chevret S, Delaunay J, Stamatoullas A, Rose C, Beyne-Rauzy O, Banos A, Guerci-Bresler A, Wickenhauser S, Caillot D, Laribi K, De Renzis B, Bordessoule D, Gardin C, Slama B, Sanhes L, Gruson B, Cony-Makhoul P, Chouffi B, Salanoubat C, Benramdane R, Legros L, Wattel E, Tertian G, Bouabdallah K, Guilhot F, Taksin AL, Cheze S, Maloum K, Nimuboma S, Soussain C, Isnard F, Gyan E, Petit R, Lejeune J, Sardnal V, Renneville A, Preudhomme C, Fontenay M, Fenaux P, Dreyfus F. Lenalidomide with or without erythropoietin in transfusion-dependent erythropoiesis-stimulating agent-refractory lower-risk MDS without 5q deletion. Leukemia 30, 897–905 (2016). [PubMed: 26500139]
36. Shiozawa Y, Sato-Otsubo S, Gallì A, Yoshida K, Yoshizato T, Sato Y, Kataoka K, Sanada M, Shiraishi Y, Chiba K, Miyano S, Malcovati L, Cazzola M, Ogawa S, Comprehensive Analysis of Aberrant RNA Splicing in Myelodysplastic Syndromes, Blood 124, 826–826 (2014).

37. Cretu C, Schmitzová J, Ponce-Salvatierra A, Dybkov O, De Laurentiis EI, Sharma K, Will CL, Urlaub H, Lührmann R, Pena V, Molecular Architecture of SF3b and Structural Consequences of Its Cancer-Related Mutations, Molecular Cell 64, 307–319 (2016). [PubMed: 27720643]
38. Quesada V, Conde L, Villamor N, Ordóñez GR, Jares P, Bassaganyas L, Ramsay AJ, Beà S, Pinyol M, Martínez-Trillos A, López-Guerra M, Colomer D, Navarro A, Baumann T, Aymerich M, Rozman M, Delgado J, Giné E, Hernández JM, González-Díaz M, Puente DA, Velasco G, Freije JMP, Tubío JMC, Royo R, Gelpí JL, Orozco M, Pisano DG, Zamora J, Vázquez M, Valencia A, Himmelbauer H, Bayés M, Heath S, Gut M, Gut I, Estivill X, López-Guillermo A, Puente XS, Campo E, López-Otín C, Exome sequencing identifies recurrent mutations of the splicing factor SF3B1 gene in chronic lymphocytic leukemia, Nature Genetics 44, 47–52 (2011). [PubMed: 22158541]
39. Gentien D, Kosmider O, Nguyen-Khac F, Albaud B, Rapinat A, Dumont AG, Damm F, Popova T, Marais R, Fontenay M, Roman-Roman S, Bernard OA, Stern M-H, A common alternative splicing signature is associated with SF3B1 mutations in malignancies from different cell lineages, Leukemia 28, 1355–1357 (2014). [PubMed: 24434863]
40. Seldin MM, Tan SY, Wong GW, Metabolic function of the CTRP family of hormones, Rev Endocr Metab Disord 15, 111–123 (2014). [PubMed: 23963681]
41. Brada SJL, de Wolf JT, Hendriks D, Louwes H, van den Berg E, Vellenga E, Characterization of the erythropoiesis in myelodysplasia by means of ferrokinetic studies, in vitro erythroid colony formation and soluble transferrin receptor, Leukemia 12, 340–345 (1998). [PubMed: 9529128]
42. Metzgeroth G, Rosée PL, Kuhn C, Schultheis B, Dorn-Beineke A, Hehlmann R, Hastka J, The soluble transferrin receptor in dysplastic erythropoiesis in myelodysplastic syndrome, European Journal of Haematology 79, 8–16 (2007). [PubMed: 17532764]
43. Ashby DR, Gale DP, Busbridge M, Murphy KG, Duncan ND, Cairns TD, Taube DH, Bloom SR, Tam FWK, Chapman R, Maxwell PH, Choi P, Erythropoietin administration in humans causes a marked and prolonged reduction in circulating hepcidin, Haematologica 95, 505–508 (2010). [PubMed: 19833632]
44. Tamary H, Shalev H, Perez-Avraham G, Zoldan M, Levi I, Swinkels DW, Tanno T, Miller JL, Elevated growth differentiation factor 15 expression in patients with congenital dyserythropoietic anemia type I, Blood 112, 5241–5244 (2008). [PubMed: 18824595]
45. Nicolas G, Viatte L, Lou D-Q, Bennoun M, Beaumont C, Kahn A, Andrews NC, Vaulont S, Constitutive hepcidin expression prevents iron overload in a mouse model of hemochromatosis, Nature Genetics 34, 97–101 (2003). [PubMed: 12704388]
46. Nemeth E, Tuttle MS, Powelson J, Vaughn MB, Donovan A, Ward DM, Ganz T, Kaplan J, Hepcidin Regulates Cellular Iron Efflux by Binding to Ferroportin and Inducing Its Internalization, Science 306, 2090–2093 (2004). [PubMed: 15514116]
47. Cui R, Gale RP, Zhu G, Xu Z, Qin T, Zhang Y, Huang G, Li B, Fang L, Zhang H, Pan L, Hu N, Qu S, Xiao Z, Serum iron metabolism and erythropoiesis in patients with myelodysplastic syndrome not receiving RBC transfusions, Leukemia Research 38, 545–550 (2014). [PubMed: 24598841]
48. Pasricha S-R, Frazer DM, Bowden DK, Anderson GJ, Transfusion suppresses erythropoiesis and increases hepcidin in adult patients with β-thalassemia major: a longitudinal study, Blood 122, 124–133 (2013). [PubMed: 23656728]
49. Malcovati L, Karimi M, Papaemmanuil E, Ambaglio I, Jädersten M, Jansson M, Elena C, Gallì A, Walldin G, Della Porta MG, Raaschou-Jensen K, Travaglino E, Kallenbach K, Pietra D, Ljungström V, Conte S, Boveri E, Invernizzi R, Rosenquist R, Campbell PJ, Cazzola M, Hellström Lindberg E, SF3B1 mutation identifies a distinct subset of myelodysplastic syndrome with ring sideroblasts, Blood 126, 233–241 (2015). [PubMed: 25957392]
50. Cazzola M, Barosi G, Gobbi PG, Invernizzi R, Riccardi A, Ascari E, Natural history of idiopathic refractory sideroblastic anemia, Blood 71, 305–312 (1988). [PubMed: 3337899]
51. Gattermann N, Finelli C, Porta MD, Fenaux P, Stadler M, Guerci-Bresler A, Schmid M, Taylor K, Vassilieff D, Habr D, Marcellari A, Roubert B, Rose C, Hematologic responses to deferasirox therapy in transfusion-dependent patients with myelodysplastic syndromes, Haematologica 97, 1364–1371 (2012). [PubMed: 22419577]

52. List AF, Baer MR, Steensma DP, Raza A, Esposito J, Martinez-Lopez N, Paley C, Feigert J, Besa E, Deferasirox Reduces Serum Ferritin and Labile Plasma Iron in RBC Transfusion–Dependent Patients With Myelodysplastic Syndrome, JCO 30, 2134–2139 (2012).

53. Meunier M, Ancelet S, Lefebvre C, Arnaud J, Garrel C, Pezet M, Wang Y, Faure P, Szymanski G, Duployez N, Preudhomme C, Biard D, Polack B, Cahn J-Y, Moulis JM, Park S, Meunier M, Ancelet S, Lefebvre C, Arnaud J, Garrel C, Pezet M, Wang Y, Faure P, Szymanski G, Duployez N, Preudhomme C, Biard D, Polack B, Cahn J-Y, Marc Moulis J, Park S, Reactive oxygen species levels control NF-kappaB activation by low dose deferasirox in erythroid progenitors of low risk myelodysplastic syndromes, Oncotarget 8, 105510–105524 (2017). [PubMed: 29285268]

54. Platzbecker U, Germing U, Götze KS, Kiewe P, Mayer K, Chromik J, Radsak M, Wolff T, Zhang X, Laadem A, Sherman ML, Attie KM, Giagounidis A, Luspatercept for the treatment of anaemia in patients with lower-risk myelodysplastic syndromes (PACE-MDS): a multicentre, open-label phase 2 dose-finding study with long-term extension study, The Lancet Oncology 18, 1338–1347 (2017). [PubMed: 28870615]

55. Suragani RNVS, Cadena SM, Cawley SM, Sako D, Mitchell D, Li R, Davies MV, Alexander MJ, Devine M, Loveday KS, Underwood KW, Grinberg AV, Quisel JD, Chopra R, Pearsall RS, Seehra J, Kumar R, Transforming growth factor-β superfamily ligand trap ACE-536 corrects anemia by promoting late-stage erythropoiesis, Nat. Med 20, 408–414 (2014). [PubMed: 24658078]

56. Dussiot M, Maciel TT, Fricot A, Chartier C, Negre O, Veiga J, Grapton D, Paubelle E, Payen E, Beuzard Y, Leboulch P, Ribeil J-A, Arlet J-B, Coté F, Courtois G, Ginzburg YZ, Daniel TO, Chopra R, Sung V, Hermine O, Moura IC, An activin receptor IIA ligand trap corrects ineffective erythropoiesis in β-thalassemia, Nat. Med 20, 398–407 (2014). [PubMed: 24658077]

57. Gardenghi S, Ramos P, Marongiu MF, Melchiori L, Breda L, Guy E, Muirhead K, Rao N, Roy CN, Andrews NC, Nemeth E, Follenzi A, An X, Mohandas N, Ginzburg Y, Rachmilewitz EA, Giardina PJ, Grady RW, Rivella S, Hepcidin as a therapeutic tool to limit iron overload and improve anemia in β-thalassemic mice, J Clin Invest 120, 4466–4477 (2010). [PubMed: 21099112]

58. Welch JJ, Watts JA, Vakoc CR, Yao Y, Wang H, Hardison RC, Blobel GA, Chodosh LA, Weiss MJ, Global regulation of erythroid gene expression by transcription factor GATA-1, Blood 104, 3136–3147 (2004). [PubMed: 15297311]

59. Roepstorff P, Fohlman J, Proposal for a common nomenclature for sequence ions in mass spectra of peptides, Biomed. Mass Spectrom 11, 601 (1984). [PubMed: 6525415]

60. Lefebvre T, Dessendier N, Houamel D, Ialy-Radio N, Kannengiesser C, Manceau H, Beaumont C, Nicolas G, Gouya L, Puy H, Karim Z, LC-MS/MS method for hepcidin-25 measurement in human and mouse serum: clinical and research implications in iron disorders, Clinical Chemistry and Laboratory Medicine (CCLM) 53, 1557–1567 (2015). [PubMed: 25781546]

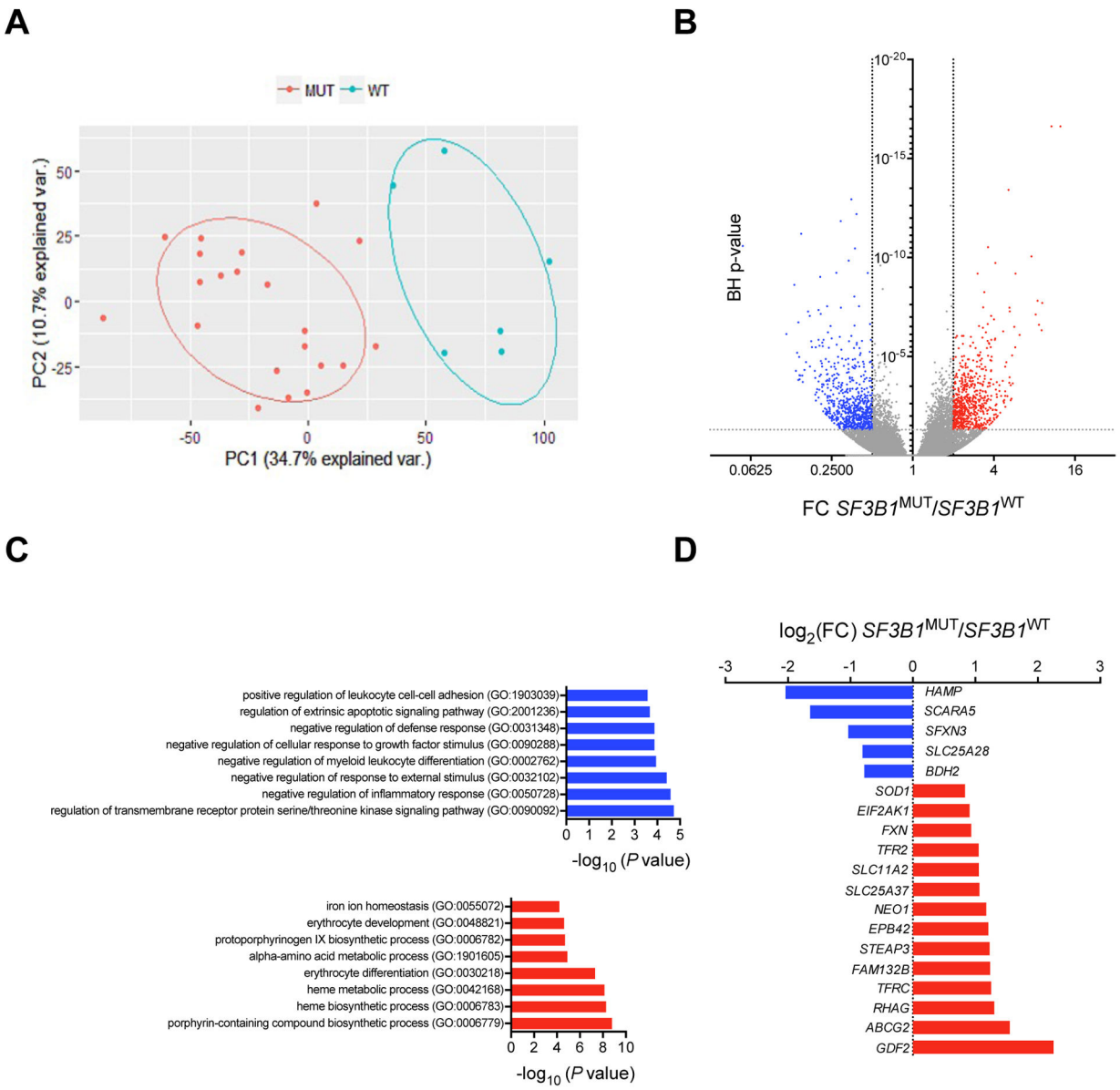

Fig. 1: Differential gene expression in *SF3B1*^{MUT} MDSs.

(**A**) Bi-plot of the first 2 principal components (PCs) showing 45.4% of the variability within the data (PC1, *x*-axis; PC2, *y*-axis). (**B**) Volcano plot showing differentially expressed transcripts in *SF3B1*^{MUT} BM MNCs compared to *SF3B1*^{WT} BM MNCs. Fold change (FC) on x-axis and negative $\log_{10}$ of Benjamini-Hochberg (BH) corrected *P*-values on y-axis. Dashed vertical and horizontal lines reflect the filtering criteria (FC <0.5 or >2.0 and BH-corrected *P*-value <0.05). The red dots represent differentially up-regulated transcripts, the blue dots represent differentially down-regulated transcripts, and the gray dots represent transcripts without differential expression. (**C**) GO enrichment analysis of differentially expressed genes with an absolute $\log_2$ (FC) >1 and a *P*-value <0.05 in *SF3B1*^{MUT} MDS. The most down-regulated and up-regulated gene sets are represented. (**D**) Log_2(FC) of the

expression of 16 among the 96 genes of the IRON_ION_HOMEOSTASIS gene set (GO:005072) deregulated in *SF3B1*^{MUT} MDS.

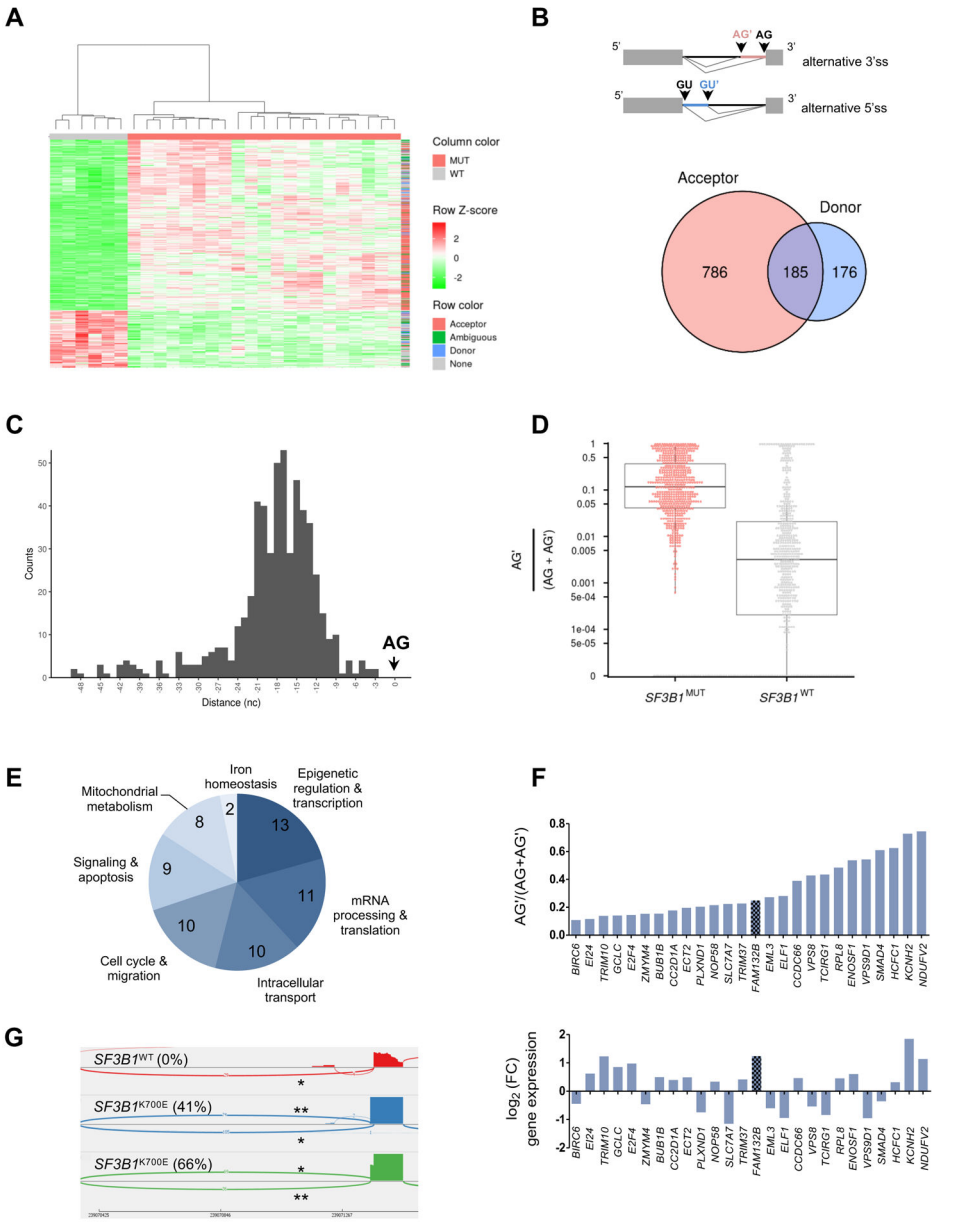

Fig. 2: Differential splice junctions in *SF3B1*^{MUT} MDSs.

(**A**) Hierarchical clustering and heat-map of differential splice junctions between *SF3B1*^{MUT} and *SF3B1*^{WT} MDS samples. Values indicating percent usage of the differential splice junction versus all other junctions sharing the same splice site are normalized as Z scores across patients and limited to a maximum of |Z| = 2. Rows are splice junctions with indicated types: acceptor (red), donor (blue), ambiguous (green), and differentially expressed canonical junction (gray). Columns are patients. (**B**) Venn diagram of the number of differential alternative 5' donor and 3' acceptor junctions in *SF3B1*^{MUT} compared to *SF3B1*^{WT} MDS. The overlapping area represents ambiguous junctions (n = 185). (**C**) Distances between the alternative (AG') and canonical (AG) 3'splice sites within the 50 nucleotides upstream of the AG plotted as a histogram. (**D**) Comparison of the expression of

alternative junctions. The ratio AG'/AG'+AG for each junction in *SF3B1*^{MUT} (red) versus *SF3B1*^{WT} (gray) MDS is shown. (**E**) Distribution of the biological functions of 63 genes affected by one or two aberrant 3'ss junctions located at <50 bases of the canonical 3'ss, an additional sequence multiple of 3 nucleotides, a ratio AG'/(AG'+AG) >0.1 in *SF3B1*^{MUT} samples, and a FC >10. (**F**) Ratio of AG'/(AG'+AG) in 26 genes whose expression was up- or down-regulated in *SF3B1*^{MUT} patients. (**G**) Sashimi plot of 3'ss canonical (*) and aberrant (**) junctions in *FAM132B/ERFE* gene in three BM MNC samples, 1 *SF3B1*^{WT} and 2 *SF3B1*^{K700E} MDS. The ratio AG'/(AG'+AG) is indicated in parentheses.

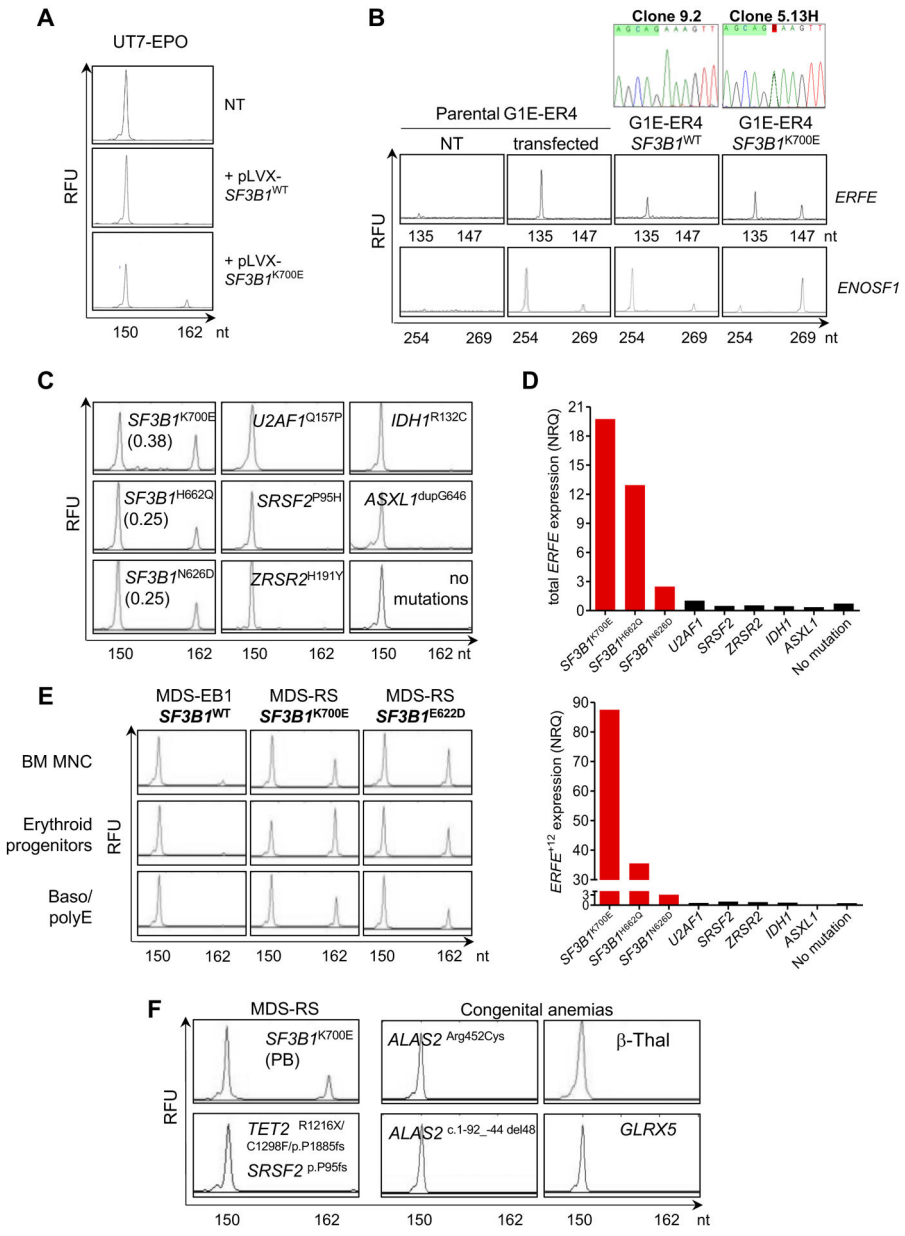

Fig. 3: *SF3B1*-dependent expression of 3'ss aberrant *ERFE*$^{+12}$.

(**A**) Induction of *ERFE*$^{+12}$ by expressing *SF3B1*^{K700E} in human *SF3B1*^{WT} UT-7/EPO cell line. Cells were transfected with a pLVX plasmid encoding a synthetic *SF3B1*^{WT} or *SF3B1*^{K700E} cDNA. Non-transfected (NT) UT-7/EPO cells are shown as a control. The canonical *ERFE* and aberrant *ERFE*$^{+12}$ transcripts were detected by capillary electrophoresis of fluorescent PCR products. The x-axis represents molecular size (nt for nucleotides) of PCR amplicons, and the y-axis represents relative fluorescent units (RFU). The peak at 150 nt corresponds to the canonical transcript, whereas the peak at 162 nt refers to the alternative transcript due to cryptic AG' usage. (**B**) Analysis of alternative AG' and canonical AG usage of *ERFE* and *ENOSF1* minigenes transfected into murine CRISPR-Cas9 *SF3B1*^{WT} (clone 9.2) and *SF3B1*^{K700E} (clone 5.13H) G1E-ER4 cells by fluorescent PCR. Transfected and NT

parental G1E-ER4 cells are shown as controls. The peak at 135 nt corresponds to the transcript generated by a canonical AG usage, whereas the peak at 147 nt refers to the alternative transcript due to cryptic AG' usage. (**C**) Detection of *ERFE*$^{+12}$ depends on the presence of a *SF3B1* mutant in MDS. BM MNC RNAs from 3 patients with *SF3B1* mutations (*SF3B1*^{K700E}, *SF3B1*^{H622Q}, *SF3B1*^{N626D}), 3 with mutations in other splice genes (*U2AF1*^{Q157P}, *SRSF2*^{P95H}, *ZRSR2*^{H191Y}), and 3 with *IDH1*^{R132C}, *ASXL1*^{dupG646} or no mutations were analyzed. *ERFE*$^{+12}$/*ERFE*$^{+12}$+*ERFE*^{WT} ratios are indicated. (**D**) Quantification of *ERFE*^{WT} and *ERFE*$^{+12}$ transcripts by RT-qPCR in BM samples depicted in (C). Results are expressed as normalized ratio quantities (NRQ) to *ACTB* and *B2M* housekeeping genes. (**E**) Detection of *ERFE*^{WT} and *ERFE*$^{+12}$ transcripts in *SF3B1*^{MUT} or *SF3B1*^{WT} erythroid progenitors or basophilic/polychromatic erythroblasts (Baso/polyE) in culture in comparison with BM MNC. (**F**) Analysis of *ERFE* transcripts in *SF3B1*^{WT} diseases with ineffective erythropoiesis. The image shows peripheral blood (PB) MNC from 1 patient with MDS-RS with *TET2*, *SRSF2* and no *SF3B1* mutations, samples from 3 patients with congenital sideroblastic anemias (2 BM samples with *ALAS2* mutation and 1 PB sample with *GLRX5* mutation) and one PB sample from a patient with severe β-thalassemia (β-Thal). Samples were analyzed by capillary electrophoresis of *ERFE* PCR products. One PB sample from a *SF3B1*^{K700E} MDS patient was used as a positive control.

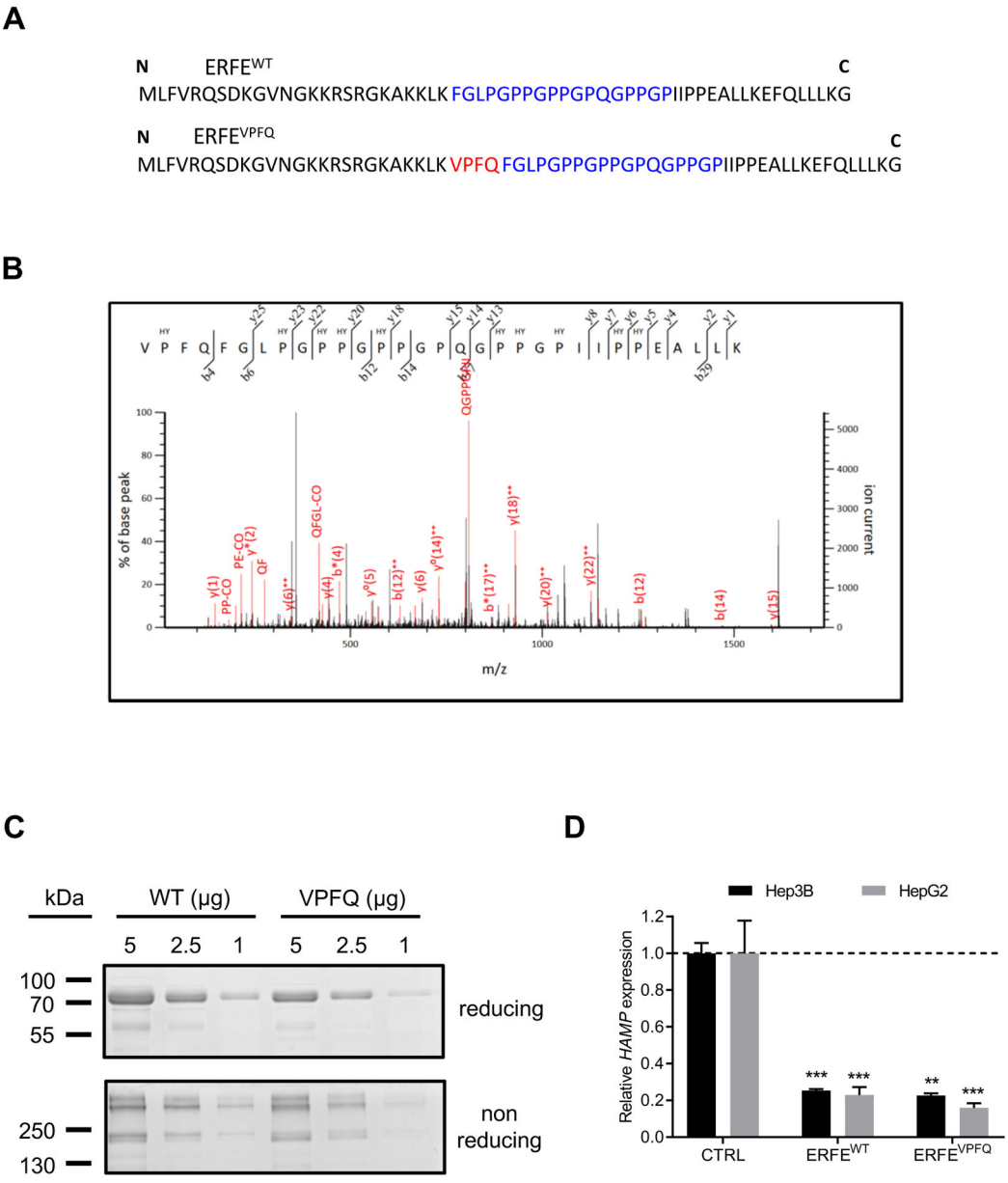

Fig. 4: Identification of ERFE^{VPFQ} peptide by mass spectrometry and hepcidin repression by recombinant ERFE^{VPFQ} protein.

(**A**) Amino-acid sequence of ERFE^{WT} and ERFE^{VPFQ} peptides. VPFQ (red), collagen domain (blue). (**B**) Identification of a specific ERFE^{VPFQ} peptide in erythroblast cell lysates by mass spectrometry using nano liquid chromatography coupled with a Q-Exactive Plus mass spectrometer. The calculated peptide mass was 3227.650782 from 3+ ion observed at m/z 1076.890870 with measured Δ = 3.6 ppm, Mascot Score = 17, expectation value = 0.069. HY: hydroxylated proline residues. (**C**) SDS-PAGE and Coomassie Blue staining of purified ERFE^{WT} and ERFE^{VPFQ} in reducing and non-reducing conditions. (**D**) Hep3B and HepG2 hepatocellular carcinoma cells were treated with 2 µg/ml of purified recombinant human ERFE^{WT} or ERFE^{VPFQ} for 16 hours. *HAMP* was quantified by RT-qPCR, and normalized to *HPRT*. Data shown are means ± SEM of three independent experiments and

represent a fold change of hepcidin mRNA expression in ERFE-treated compared to untreated (CTRL) cells. Two-tailed Student t-test for *P*-values; *** $P<0.0001$; ** $P<0.001$.

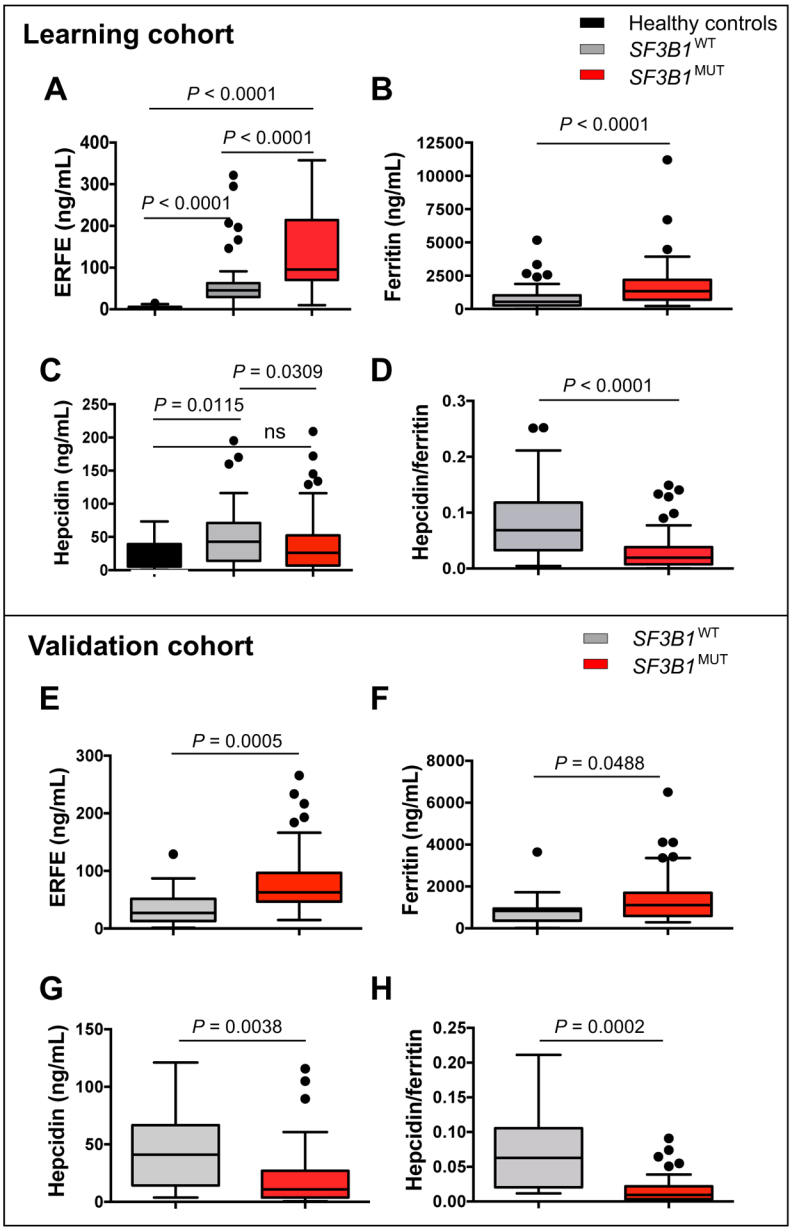

Fig. 5: Increased plasma concentration of ERFE in *SF3B1*^{MUT} MDS patients.

Quantitative analysis was performed in plasmas collected from 20 non-blood donor healthy volunteers (black), 156 patients with MDS including 94 *SF3B1*^{MUT} (red) and 62 *SF3B1*^{WT} (gray) representing the training cohort (**A-D**), and 55 patients with MDS including 42 *SF3B1*^{MUT} (red) and 13 *SF3B1*^{WT} (gray) representing the validation cohort (**E-H**). The graphs show quantification of erythroferrone (**A, E**), ferritin (**B, F**), hepcidin (**C, G**), and hepcidin/ferritin ratio (**D, H**). Results are expressed as medians and interquartile ranges (IQRs). The boxplots represent the median and the first and third quartiles, and the whiskers represent the lowest and the highest values still within the 1.5 IQR of the lower and upper quartiles. Mann-Whitney for *P*-values.

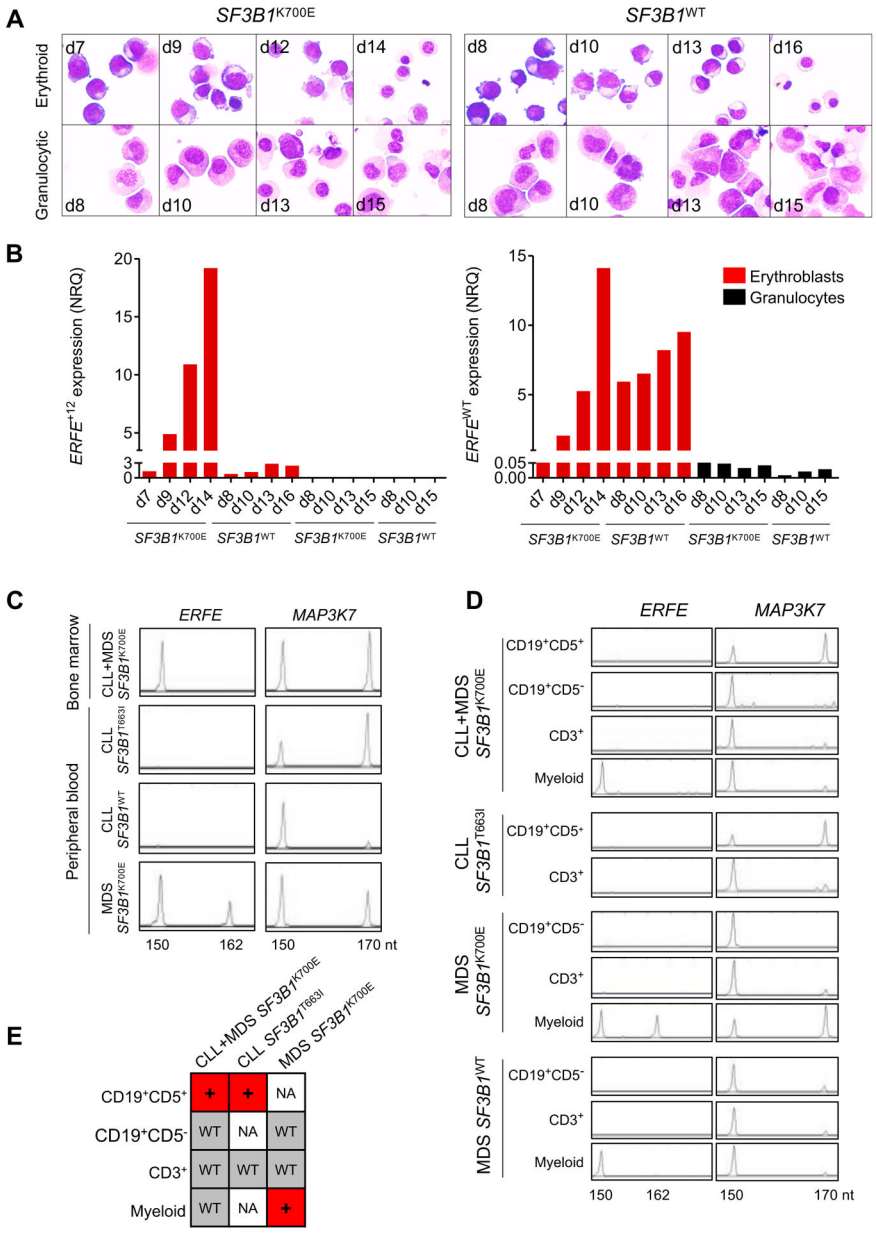

Fig. 6: Erythroid cell-restricted expression of *ERFE*$^{+12}$.

(**A**) May-Grünwald-Giemsa-stained cytospins of erythroid and granulocytic precursors obtained from liquid culture of BM *SF3B1*^{WT} or *SF3B1*^{K700E} CD34^{+} progenitors. (**B**) Quantification of *ERFE*^{WT} and *ERFE*$^{+12}$ in erythroid and granulocytic precursors by RT-qPCR. Results are expressed as NRQ ± SEM to *ACTB* and *B2M* housekeeping genes. (**C**) *ERFE*$^{+12}$ is absent in *SF3B1*^{MUT} CLL. BM MNCs from a patient with *SF3B1*^{K700E} CLL +MDS or PB MNCs from patients with *SF3B1*^{T663I} CLL, *SF3B1*^{WT} CLL, and *SF3B1*^{K700E} MDS were collected for analysis by capillary electrophoresis of *ERFE* and *MAP3K7* fluorescent PCR products. *ERFE*$^{+12}$ was detected as a 162-nt fragment and *MAP3K7*$^{+20}$ as a 170-nt fragment. PB samples from one patient with an *SF3B1*^{WT} CLL and one patient with an *SF3B1*^{MUT} MDS are shown as controls. (**D**) *ERFE*$^{+12}$ expression is restricted to

SF3B1^{MUT} myeloid lineage. CD19^{+}CD5^{-} B cells, CD19^{+}CD5^{+} B CLL cells, CD3^{+} T cells, and myeloid cells were sorted from the BM MNC fraction of a *SF3B1*^{K700E} CLL+MDS, a *SF3B1*^{K700E} MDS, and a *SF3B1*^{WT} MDS and from the PB MNCs of a *SF3B1*^{T663I} CLL *ERFE* and *MAP3K7* transcripts were analyzed by fluorescent PCR. (**E**) The sequencing of *SF3B1* was performed on cDNA of each cell fraction. +: mutated; WT: wild type; NA: not available.

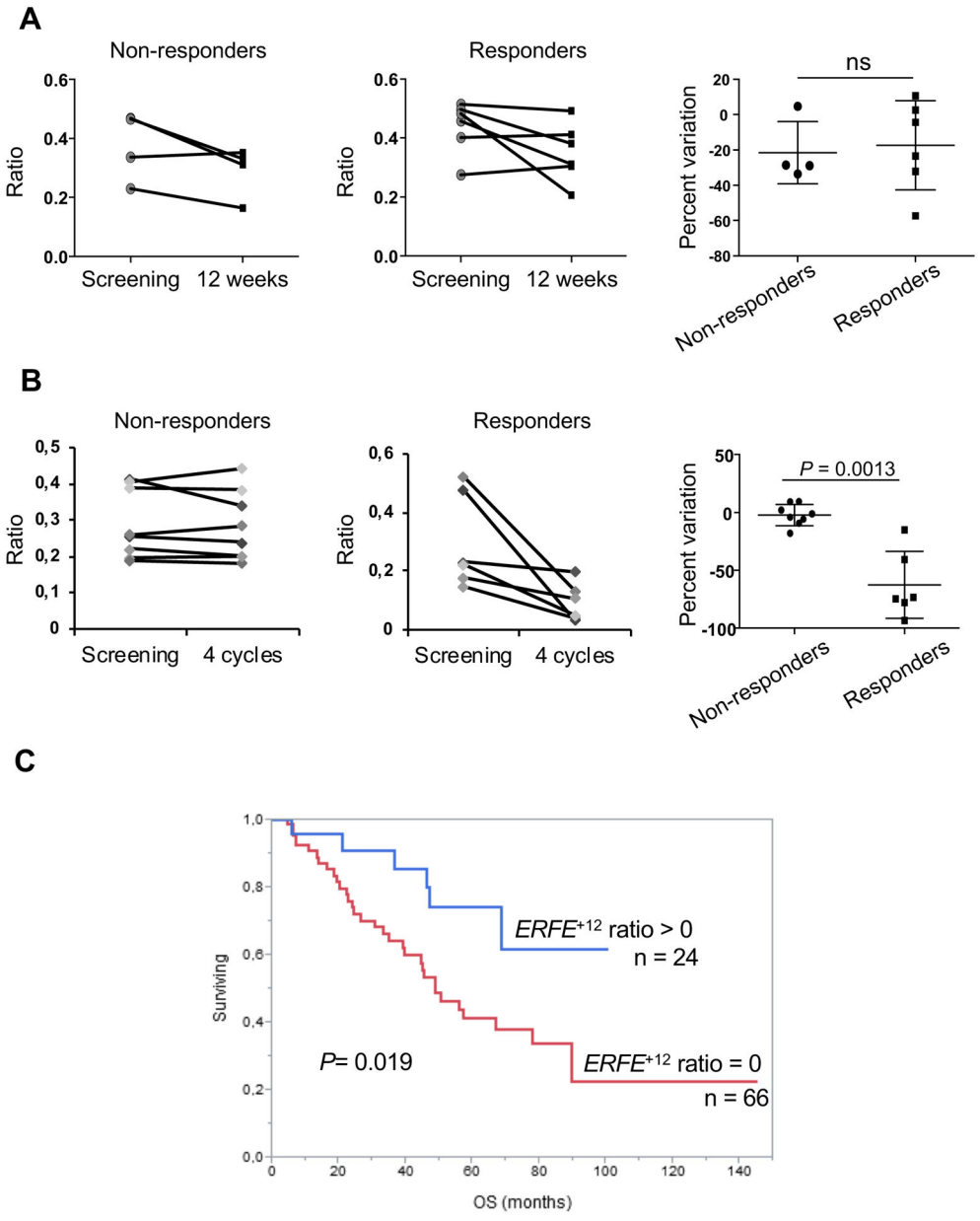

Fig. 7: *ERFE*$^{+12}$ expression as a marker of clonal erythropoiesis and survival.

Fluorescent PCR was performed at screening and evaluation in (**A**) 10 paired samples from *SF3B1*^{MUT} MDS patients enrolled in the GFM-Retacrit-2013 clinical trial (4 non-responding and 6 responding patients) and (**B**) 14 paired samples from patients with *SF3B1*^{MUT} MDS enrolled in the GFM-LenEpo-2008 clinical trial (8 non-responding and 6 responding patients). Peak heights of *ERFE*$^{+12}$ and *ERFE*^{WT} signals were integrated as *ERFE*$^{+12}$/*ERFE*$^{+12}$+*ERFE*^{WT} ratios. Percent variations of ratios are indicated (right) as medians and IQR (25 – 75%). Mann-Whitney test for *P*-values. (**C**) Overall survival according to *ERFE*$^{+12}$/*ERFE*$^{+12}$+*ERFE*^{WT} ratio shown as a Kaplan-Meier curve. A

threshold of positivity of 0.008 was determined by ROC analysis. Log-Rank test for *P*-value. ns: not significant.

Table 1:

Erythroferrone, hepcidin and *SF3B1* mutation as independent predictors of hyperferritinemia in low transfusion burden MDS patients. Erythroferrone, hepcidin, sTfR, number of RBC units per 8 weeks, and *SF3B1* mutation were evaluated in the group of 60 patients receiving less than 4 RBC units per 8 weeks on the basis of ferritin with a cut-off value of 300 ng/ml. Parameters are indicated as means and 95% confidence intervals (95% CI) or ranges. For univariate analysis, Mann-Whitney and X^2 tests were used to compare the variables between $SF3B1^{MUT}$ and $SF3B1^{WT}$ MDS. Multivariate logistic regression analysis was performed for variables with *P*-value <0.100 in univariate analysis.

Parameters	Ferritin < 300 ng/ml	Ferritin ≥ 300 ng/ml	Univariate	Multivariate
	n = 19	n = 41	*P*-value	*P*-value
Erythroferrone (ng/ml), mean (95% CI)	36.7 (26.8 – 46.6)	72.7 (55.4 – 90.0)	0.005	0.002
Hepcidin (ng/ml), mean (95% CI)	17.2 (11.2 – 23.2)	35.9 (25.9 – 45.9)	0.013	<0.0001
sTfR (ng/ml), mean (95% CI)	1.21 (0.99 – 1.43)	1.42 (1.18 – 1.65)	0.484	
Number of RBC units / 8 weeks, mean (range)	0.2 (0 – 2)	0.6 (0 – 3)	0.104	
***SF3B1* mutation yes, n (%)**	3 (15.8)	22 (53.6)	0.006	0.023